JOURNAL OF VIROLOGY, Sept. 2006, p. 8329–8344 Vol. 80, No. 17
0022-538X/06/$08.00+0 doi:10.1128/JVI.00540-06

Tobacco Mosaic Virus Movement Protein Functions as a Structural Microtubule-Associated Protein

Jamie Ashby,[2,3]† Emmanuel Boutant,[1]† Mark Seemanpillai,[1]† Adrian Sambade,[1] Christophe Ritzenthaler,[1] and Manfred Heinlein[1,2,3]*

Institut de Biologie Moléculaire des Plantes, 12 Rue du Général Zimmer, 67084 Strasbourg, France[1]; Botanisches Institut der Universität Basel, Hebelstrasse 1, 4056 Basel, Switzerland[2]; and Friedrich Miescher Institute for Biomedical Research, Maulbeerstrasse 66, 4058 Basel, Switzerland[3]

Received 15 March 2006/Accepted 4 June 2006

The cell-to-cell spread of *Tobacco mosaic virus* infection depends on virus-encoded movement protein (MP), which is believed to form a ribonucleoprotein complex with viral RNA (vRNA) and to participate in the intercellular spread of infectious particles through plasmodesmata. Previous studies in our laboratory have provided evidence that the vRNA movement process is correlated with the ability of the MP to interact with microtubules, although the exact role of this interaction during infection is not known. Here, we have used a variety of in vivo and in vitro assays to determine that the MP functions as a genuine microtubule-associated protein that binds microtubules directly and modulates microtubule stability. We demonstrate that, unlike MP in whole-cell extract, microtubule-associated MP is not ubiquitinated, which strongly argues against the hypothesis that microtubules target the MP for degradation. In addition, we found that MP interferes with kinesin motor activity in vitro, suggesting that microtubule-associated MP may interfere with kinesin-driven transport processes during infection.

Higher eukaryotes have developed sophisticated strategies that allow them to regulate cellular and developmental events by the selective trafficking and localization of RNA (for a review, see references 78 and 82). Several examples of intercellular and long-distance RNA movement have been described for higher plants, and of these, RNA viruses have become the subject of extensive investigation with regard to the molecular mechanisms that govern intercellular macromolecular trafficking (40). Exemplified by *Tobacco mosaic virus* (TMV) and other model viruses, RNA viruses facilitate the spread of their genomes by targeting plasmodesmata (Pd), membrane-lined pores that provide cytoplasmic continuity between adjacent cells and tissues (40, 65). Like other plant viruses, TMV encodes a movement protein (MP) that interacts with Pd and facilitates the intercellular passage of its genome (28, 39, 64). The MP modulates the size-exclusion limit (SEL) of the Pd (107) and also binds single-stranded nucleic acids in vitro to form an unfolded, elongated ribonucleoprotein complex with apparent dimensions compatible with translocation through dilated Pd (22, 23, 53). The coat protein (CP) of TMV is dispensable for cell-to-cell movement (26, 96), which is consistent with the transport of viral RNA (vRNA) in a nonencapsidated form (39). Since microinjected MP spreads rapidly between cells (77, 103) and plants themselves encode proteins thought to be functionally analogous to viral MPs (65, 108), the function of MP may directly reflect mechanisms of macromolecular Pd transport in normal plants which are exploited by viruses for the movement of their genomes. Elucidating the regulation and mechanism of MP-mediated RNA trafficking at the cellular and molecular level thus should reveal new paradigms to study systemic gene regulation.

The targeting of the MP to Pd is independent of infection and results in the deposition of fibrous material within the Pd cavity (30, 70). However, this in itself seems not to be sufficient to drive movement of TMV vRNA. For example, several MP mutants have been described which accumulate in Pd but are dysfunctional with respect to vRNA movement (11, 13, 49). Moreover, sink tissues with Pd characterized by large SELs still require MP for intercellular transport of vRNA (80). Since neither the presence of MP in Pd nor an increased SEL of the channel appear to be sufficient for virus movement, the MP is likely to perform additional functions to facilitate the transport of vRNA. To search for such additional MP functions, previous studies made use of TMV derivatives expressing a functional MP fused to green fluorescent protein (GFP). These studies revealed that, in addition to Pd, the MP also interacts with several other subcellular sites, such as the cortical endoplasmic reticulum (ER), the cytoskeleton, and peripheral "punctate structures" (39, 41, 42, 68, 81, 86).

The localization of MP with ER membranes is consistent with results of several studies indicating that ER membranes act as sites for virus replication and virus protein synthesis (6, 42, 76). During infection, ER membranes aggregate to form inclusions that function as virus factories (42, 86) or virus replication complexes (6) that contain vRNA in addition to replicase and MP (66). Although ER aggregation appears to be correlated with the presence of MP (66, 86), the accumulation of MP in these inclusions (42) is not required for replication and vRNA movement (13, 69). Nevertheless, evidence for a role of the viral replicase in cell-to-cell movement (44, 45, 47, 54, 55) suggests that the processes of virus replication and movement are functionally linked. This view is in agreement

* Corresponding author. Mailing address: Institut de Biologie Moléculaire des Plantes, 12, rue du Général Zimmer, 67084 Strasbourg, France. Phone: 33 3 88 417 258. Fax: 33 3 88 614 442. E-mail: manfred.heinlein@ibmp-ulp.u-strasbg.fr.

† Contributed equally to this work.

with observations implicating large membrane-associated complexes that contain components of the replication machinery in vRNA movement within and between cells (6, 51).

The observed associations of MP with microtubules (41, 68) and actin microfilaments (68) suggest an involvement of cytoskeletal elements in cell-to-cell movement of vRNA (19, 41, 110). Such a role for the cytoskeleton is consistent with observations in many different biological systems that the coordinated activities of cytoskeletal components are responsible for the specific transport and anchoring of RNAs (82). Actin is associated with the ER (60) as well as with Pd (1), and since the ER is continuous through the channel (40), it is conceivable that actin filaments support myosin-driven vRNA movement from ER-associated replication sites through the Pd channel. Consistent with this model, treatment of plant tissues with actin-depolymerizing agents was reported to interfere with the cell-to-cell progression of virus infection (51), although filamentous actin was recently shown to be dispensable for the localization of MP to Pd (84), again indicating that cell-to-cell movement and Pd gating functions of TMV may be independent processes.

Except for a role in cell plate formation and pollen tube organelle movements (17, 88, 89), there is little experimental evidence for involvement of microtubules in the trafficking of subcellular components in higher plants (36, 56). Thus, it was surprising that the MP-GFP so obviously decorated the cortical microtubule network (41, 42). However, a role for microtubules in vRNA movement has gained support by various in vivo studies. Using infected protoplasts and a combination of antibody labeling and in situ hybridization procedures, Más and Beachy (66) showed that vRNA localizes to microtubules in an MP-dependent manner. A subsequent study, again in protoplasts, demonstrated that vRNA is mislocalized in cells expressing a mutant MP (TAD5) (49) that binds vRNA but fails to associate with microtubules (67). Other in vivo studies using TMV derivatives encoding functional, dysfunctional, and temperature-sensitive mutants of MP fused to GFP indicated that the ability of MP to align with microtubules is not required for the targeting of MP to Pd but is nevertheless correlated with the intercellular spread of infection (10–13, 57). These studies reveal a correlation between the ability of MP-GFP to associate with microtubules and the ability of MP to spread infection, although the direct role of the complex in viral movement remains unknown. Here, we present evidence that MP binds to microtubules directly and is a genuine microtubule-associated protein (MAP) that leads to the stabilization of microtubules during later stages of infection. We also show that microtubule-associated MP is not ubiquitinated, an observation which is in disagreement with the previous proposal that microtubules are involved in the degradation of MP (35, 66, 81, 86). Rather, based on the finding that MP inhibits kinesin-driven motility in vitro, we propose that, while unlikely to be involved in the early movement functions of TMV, the intrinsic ability of MP to associate with microtubules may interfere with motor-based trafficking during late infection.

MATERIALS AND METHODS

Constructs. The construction of pTMV-MP:GFP5 (pTf5-nx2), pTMV-MP$^{\Delta C55}$:GFP5, and TMV-MP^{P81S}:GFP5 (pTf5-PS) is described elsewhere (10, 13). Plasmids pTMV-MP:GFP5 (pTf5-nx2) and pTMV-MP^{P81S}:GFP5 (pTf5-PS) encode MP-GFP (Δ10) fusion proteins carrying a deletion of the 10 C-terminal amino acids of MP. The deletion was originally introduced as a consequence of deleting the subgenomic CP promoter to avoid expression of free GFP. The deleted amino acids are not required for function or subcellular localization of MP. The construction of *Escherichia coli* expression vector pQ-MP:H_6 encoding the MP (Δ10) open reading frame (ORF) with six C-terminally fused tandem histidine residues is described elsewhere (10). To construct plasmid pTA-MP:GFP for dexamethasone-inducible expression of MP-GFP in BY-2 cells, the NruI-Acc65I fragment of plasmid pTMV-MP:GFP5 was inserted into PvuII-Acc65I-digested plasmid pBAD/MCS (A. Geerlof, EMBL protein expression and purification facility). The MP-GFP (Δ10) open reading frame was excised with XhoI and inserted into plasmid pTA7002 (5) previously digested with the same enzyme. To produce pTMV-MP:H_6:GFP, a double-stranded DNA fragment encoding six tandem histidine residues and containing 5′ SalI and 3′ BlnI restriction sites was produced by annealing specific oligonucleotides. The SalI-BlnI fragment of plasmid pTMV-MP:GFP5 was subsequently replaced with this linker, resulting with an in-frame GS$(H)_6$ insertion proximal to the C terminus of MP (Δ10). Similarly for pTMV-MP:GFP:H_6, a double-stranded DNA oligonucleotide coding for $-R(H)_6$ was substituted for the NotI-XhoI fragment of pTf5-nx2. The TMV-MP-monomeric red fluorescent protein 1 (mRFP1) variant was produced by replacing the NruI-XhoI fragment of pTf5-nx2 with a NruI-XhoI fragment comprising full-length MP (GenBank accession number 9626125) fused upstream to an mRFP1 ORF (18). A number of silent point mutations were introduced into the MP ORF at MP coordinates 786 (C to A), 789 (C to A), and 801 (G to T) to suppress the CP subgenomic promoter activity located within the 3′ end of TMV MP. Furthermore, the stop codon of the MP and the start codon of mRFP1 ORFs were replaced by the linker sequence 5′-CGGTGGTC GACGCGCGCCTAGGG-3′, which harbors a SalI restriction site. The MP ORF was excised by NruI-SalI digestion and replaced with an NruI-SalI fragment harboring the MP sequence of pTf5-nx2. Construction of Man1-mRFP-expressing plasmid pBP30-GmMan1:RFP is described elsewhere (109). To construct pGII-Ω-35S-MPΔC55:GFP for transient expression of MP$^{\Delta C55}$-GFP in BY-2 cells, an expression cassette containing the *Cauliflower mosaic virus* 35S promoter sequence, TMV omega (Ω) leader sequence, multiple cloning site, and *Cauliflower mosaic virus* 35S terminator sequence was excised with HindIII and XmaI (Klenow filled) from the modified pCambia vector p35SΩHA1300 (unpublished) and introduced into HindIII and ApaI (Klenow filled)-digested binary vector pGREEN0029 (now pGII-Ω-35SHA). The MP$^{\Delta C55}$-GFP coding sequence containing the in-frame stop codon of GFP was subsequently amplified by PCR from vector Tf5-dMP(C55)-GFP (13) and positionally cloned into NdeI/SpeI-digested pGII-Ω-35SHA. Construction of plasmid pK7WGF2-AT2g38720, for the stable expression of *Arabidopsis* GFP–MAP65-5 in BY-2 cells is described elsewhere (99).

Infection of plants and protoplasts. *Nicotiana benthamiana* plants (5 to 6 weeks old) were mechanically inoculated on expanded leaves using infectious RNA derived from in vitro transcription reactions. Plants were maintained at 70% humidity at 22°C during the 16-h photoperiod and at 20°C during the dark period. Alternatively, plants were maintained under glasshouse conditions (18 to 25°C) at 50% humidity with a minimum 16-h photoperiod. Protoplasts of suspension cell line BY-2 were prepared and inoculated by electroporation with infectious transcripts as described previously (42).

Treatments with microtubule antagonists. In planta treatment of expanding TMV infection sites with 20 μM oryzalin was performed as described previously (35). For amiprofos-methyl (APM) infiltrations, excised leaf disks containing infection foci were vacuum infiltrated with 50 μM APM and subsequently floated on the same solution under glasshouse conditions. For treatment of BY-2 protoplasts, 50 μM APM or 10 μM oryzalin was added directly to the protoplast growth medium. For measurement of infection expansion rates, drug- or water-infiltrated leaf disks containing TMV-MP-GFP infection sites (at least 30 per sample) were photographed daily using a Canon EOS 300D digital camera, and estimates of infection site diameters were determined from calibrated digital images using Adobe Photoshop software (v7.0). Immunoblot analysis of drug-infiltrated infection site proteins was performed as previously described (12).

Transformation and immunolabeling of BY-2 culture cells. BY-2 (*Nicotiana tabacum* cv. bright yellow 2) cell cultures transgenic for GFP–MAP65-5 or MP-GFP were established by *Agrobacterium tumefaciens*-mediated transformation (24) using the plasmids pK7WGF2-AT2g38720 (99) and pTA-MP:GFP, respectively. Expression of MP-GFP from pTA-MP:GFP in the transgenic cell line was induced by the addition of 10 μM dexamethasone (Sigma) directly to the BY-2 culture medium. Transient coexpression of MP$^{\Delta C55}$-GFP from plasmid pGIIΩMPΔC55:GFP and Man-1–mRFP from pBP30-GmMan1:RFP was achieved by biolistic bombardment as described previously (101). BY-2 suspension culture cells were fixed and immunostained according to the method de-

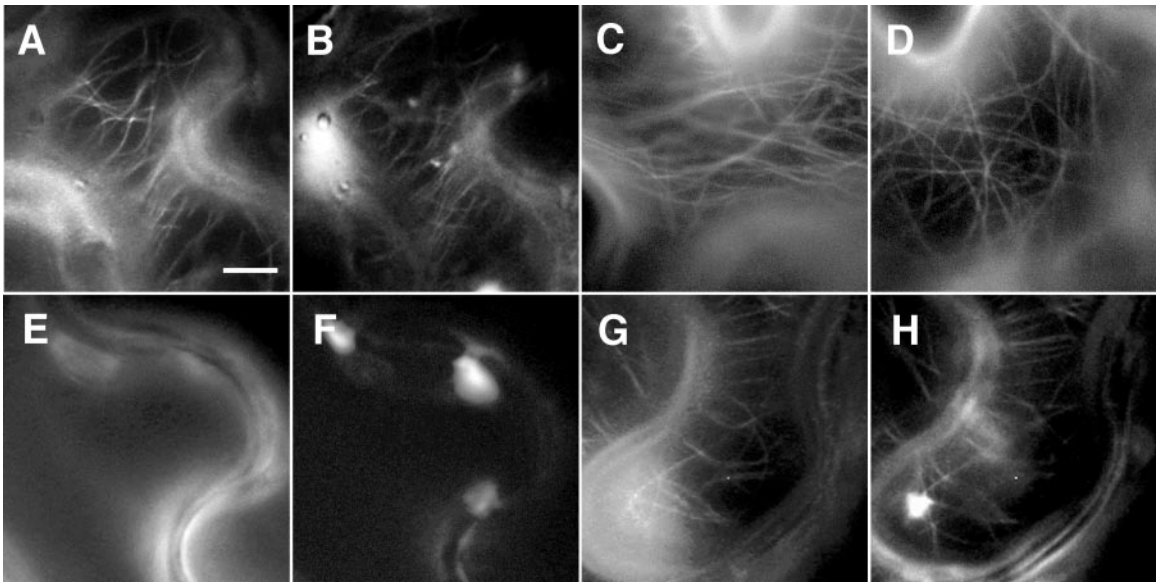

FIG. 1. MP confers increased resistance to microtubule-destabilizing drugs in planta. Transgenic *N. benthamiana* plants expressing *tua*-GFP were infected with TMV-MP-mRFP1, and cells undergoing different stages of infection were analyzed by fluorescence microscopy before and after infiltration with 20 μM oryzalin. (A and B) In untreated cells undergoing later stages of infection, MP-mRFP1 (B) clearly associates with *tua*-GFP-labeled microtubules (A). (C) *tua*-GFP-labeled microtubules are readily apparent in noninfected, noninfiltrated control cells. (D) Mock infiltration with water does not disrupt *tua*-GFP-labeled microtubules in noninfected cells. (E and F) In cells at the front of the radially expanding TMV-MP-mRFP1 infection site, infiltration with oryzalin for 30 min leads to disruption of *tua*-GFP-labeled microtubules (E) and no association of MP-mRFP1 with microtubules can be observed (F). (G and H) Following treatment for 30 min with oryzalin, MP-mRFP1 (H) remains associated with stable *tua*-GFP-labeled microtubules (G) in cells behind the front of infection. Bar, 15 μm.

scribed in reference 87, except that cell wall digestion was performed for 10 min and that mouse monoclonal anti-α-tubulin (clone DM1B, dilution 1:1,000) was used as a primary antibody. Secondary goat-anti mouse antibodies conjugated to Alexa fluor 568 were purchased from Molecular Probes.

Microscopy. Epifluorescence microscopy of infection sites, leaf epidermis, protoplasts, immunostained cytoskeletal complexes, and motor protein assays was performed with Nikon Eclipse E800 and Nikon Eclipse 80i microscopes equipped with CFI Plan Apochromat objectives (Nikon Corp.) and filter sets for visualization of GFP/Alexa fluor 488/fluorescein isothiocyanate and rhodamine/Alexa fluor 568 fluorescence, respectively. Images were acquired either with a Nikon Eclipse DXM1200 digital camera (mounted on the Nikon Eclipse E800) and Nikon ACT-1 software (Fig. 1) or with a Hamamatsu ORCA-100 progressive scan interline charge-coupled device camera (mounted on the Nikon Eclipse 80i) and Openlab software (Improvision).

For confocal laser scanning microscopy of BY-2 cells, fixed cells were mounted in a chamber containing phosphate-buffered saline, whereas living cells were allowed to settle onto a poly-L-lysine-coated coverslip which then was mounted in an Attofluor cell chamber (Invitrogen). Cells were observed with a Zeiss (Jena, Germany) LSM510 laser scanning confocal microscope using a C-Apochromat (63×; 1.2 W Korr) water objective lens under multitrack mode. Excitation/emission wavelengths were 488 nm/505 to 545 nm for GFP and 543/long pass 560 nm for Alexa fluor 568 and mRFP. LSM 510 three-dimensional reconstruction functions were employed to compute projections of serial confocal sections. For fluorescence recovery after photobleaching (FRAP) analyses, three imaging scans of the area of interest were performed, and then a specific region was selected for bleaching. Twenty bleaching iterations were performed with 70% laser power and 100% transmittance. Then scans were taken every 10 to 60 s during the course of fluorescence recovery until the fluorescence intensity reached a plateau. Images were processed using LSM510 version 2.8 (Zeiss), ImageJ (1.32j), and Adobe Photoshop v7.0 (final image assembly; Adobe Systems, Inc.). For analysis of Man1-mRFP-labeled Golgi stacks, a series of single images were obtained at known time intervals by confocal laser scanning microscopy from BY-2 cells cotransformed with plasmids pBP30-GmMan1:RFP and pGIIΩMPΔC55:GFP. The relative velocities of Golgi stacks translocating across linear trajectories were subsequently determined using Leica LSM Image browser software (v 3.5).

Preparation and analysis of plant cytoskeleton extracts. Cytoskeleton-enriched fractions were isolated from infected BY-2 protoplasts according to the method of Chan et al. (21). For immunoblot analysis of cytoskeleton proteins, cytoskeleton-enriched fractions (25 μg) were separated by electrophoresis on 12.5% sodium dodecyl sulfate (SDS)–polyacrylamide gels, transferred onto polyvinylidene difluoride membranes (Bio-Rad laboratories), and after incubation with primary antibodies against MP (amino acids 6 to 22), α-tubulin (Oncogene Research Products) or ubiquitin (Stressgen Biotechnologies), membranes were probed with peroxidase-conjugated secondary antibody (Jackson ImmunoResearch) and detected with SuperSignal West Dura extended-duration substrate (Pierce Biotechnology). For direct immunolabeling of microtubules, cytoskeleton-enriched fractions were resuspended in 100 μl of cytoskeleton extraction buffer [50 mM piperazine-N,N′-bis(2-ethanesulfonic acid) (PIPES)–OH, pH 6.9, 0.4 M mannitol, 5 mM EGTA, 5 mM $MgSO_4$, 10% dimethyl sulfoxide (DMSO), 0.05% NP-40, and 2% Triton X-100], and 20 μl of protein suspension was fixed in 100 μl of the same buffer containing 6% paraformaldehyde for 10 min at room temperature. Fixed proteins were transferred to poly-L-lysine-coated glass slides (Sigma) in a Shandon Cytospin 3 for 2 min at 2,000 rpm, and following incubation with a primary antibody against α-tubulin (Oncogene Research Products) and rhodamine-conjugated secondary antibody (Pierce Biotechnology), samples were analyzed by fluorescence microscopy as described previously (11).

In vitro microtubule binding assays. The purification of recombinant MP-H_6 is described in detail elsewhere (10). Purified bovine brain tubulin heterodimers (Cytoskeleton, Inc.) were polymerized for 45 min at 37°C in 10-μl reaction mixtures containing 5 mg/ml tubulin, 80 mM PIPES-OH (pH 6.9), 1 mM EGTA, 10% DMSO, 1 mM $MgCl_2$, and 1 mM GTP. To suppress microtubule dynamics, paclitaxel (Taxol; Sigma) was added to a final concentration of 50 μM and microtubules were incubated for 12 h at room temperature. To remove nonpolymerized tubulin, microtubules were twice collected by sedimentation at 20,800 × *g* for 5 min at room temperature and resuspended in 60 μl of microtubule binding buffer (12 mM PIPES-OH pH 6.9, 0.5 mM $MgCl_2$, 10% glycerol, 0.01% Tween 20, and 10 μM paclitaxel). Aliquots of the microtubules were heat denatured and quantified with the BCA protein assay kit (Pierce Biotechnology). MP:H_6 (in 12.5 mM PIPES-OH, pH 6.9) was thawed on ice and cleared of particulate material by centrifugation at 100,000 × *g* for 30 min in a Beckman TLA-100 ultracentrifuge at 4°C. Following quantification of protein concentration, increasing amounts of MP-H_6 (0.1 to 10 mM) were incubated for 10 min at room temperature with 2.0 mM polymerized tubulin dimers in microtubule binding buffer (25 μl). Microtubules and associated MP-H_6 were collected by sedimentation at 20,800 × *g* for 10 min at room temperature, and both the pellet and

supernatant fractions were visualized by 12.5% SDS–polyacrylamide gel electrophoresis and colloidal Coomassie blue staining. In control experiments, a 1.5 μM concentration of either GST-H_6 (kindly provided by J. Hofsteenge) or bovine serum albumin (BSA; Pierce Biotechnology) was incubated with 6 μM polymerized tubulin and analyzed as described above. Replicate gels from microtubule binding assays were digitized using a Typhoon 9400 variable-mode imager (Amersham Biosciences), and images were imported into Quantity One 4.5.0 analysis software (Bio-Rad Laboratories). A standard curve was produced from densitometric readings of known MP-H_6 amounts (0.1 to 30 μM), and the amounts of microtubule-associated MP-H_6 ($[MP]_{bound}$) and unbound MP-H_6 ($[MP]_{free}$) were estimated from the standard curve and adjusted for nonspecific sedimentation of MP-H_6 in the absence of tubulin. Values for $[MP]_{bound}$ were plotted versus $[MP]_{free}$, yielding a saturation hyperbole, and values for binding stoichiometry ($n = [MP]_{bound}/[\text{tubulin dimer}]$) and the dissociation constant (K_D) were calculated by nonlinear regression according to a noncatalytic ligand-receptor binding model (2). For stability assays, 3.0 μM polymerized, paclitaxel-stabilized tubulin was incubated with increasing amounts of MP-H_6 for 30 min at 4°C in microtubule-destabilizing buffer (12 mM PIPES-OH, pH 6.9, 0.2% DMSO, and 10 mM $CaCl_2$), and microtubule-associated and free proteins were subsequently separated by sedimentation and analyzed by SDS-PAGE and colloidal Coomassie blue staining. For salt stability assays, 2.0 μM polymerized, paclitaxel-stabilized tubulin was incubated in microtubule binding buffer with a 1.5 μM concentration of either MP-H_6 or recombinant H_6-*Tau* protein (Panvera) in reaction mixtures containing varying amounts of NaCl. After incubation for 10 min at room temperature, protein complexes were analyzed as described above. For immunostaining and microscopic analysis of MP-H_6-associated microtubule complexes formed in the in vitro reactions, the complexes were collected by centrifugation and subsequently spun onto polylysine-coated slides using a Shandon cytocentrifuge, fixed, double labeled with antibodies against MP and α-tubulin (Oncogene Research Products), and visualized by fluorescence microscopy as described above.

Kinesin motor assays. Perfusion chambers were fabricated by placing two 50-mm strips of Scotch tape lengthwise along a plain glass slide with a 6-mm gap between strips. An 18-mm-square glass coverslip was attached to the tape strips with transparent nail varnish, resulting in a chamber volume of 8 ± 2 μl. Chambers were coated for 3 min at room temperature with 10 μl of casein (0.25 mg/ml) and human glutathione *S*-transferase (GST)-conjugated kinesin 1 heavy chain (50 μg/ml; Cytoskeleton, Inc.) in motility buffer (50 mM PIPES-OH, pH 6.9, 1 mM EGTA, 2 mM $MgCl_2$, 10 μM paclitaxel, 10% glycerol). An equal mixture of rhodamine-labeled and unlabeled bovine brain tubulins (Cytoskeleton, Inc.) was polymerized as described above, and 50 μl of polymer solution (12.5 μg/ml or 110 nM polymerized dimers) was perfused through the chamber and incubated for 2 min at room temperature. Unbound microtubules were removed with 50 μl of motility buffer, followed by 100 μl of microtubule binding buffer (12 mM PIPES-OH, pH 6.9, 0.5 mM $MgCl_2$, 10% glycerol, 0.01% Tween 20, and 10 μM paclitaxel) before various concentrations of MP, BSA, or GST (all in microtubule binding buffer) were perfused through the chamber (50 μl) and incubated for 10 min at room temperature. Perfusion chambers were washed with 50 μl of motility buffer and placed on the stage of a Nikon Eclipse E800 microscope, and fluorescent microtubules on the upper surface of the chamber were visualized using a G-2A (Nikon) filter set and a 60× oil immersion objective. To initiate kinesin motor activity, 100 μl of motility buffer containing 2 mM ATP was perfused through the chamber and images of microtubule movements were recorded at known intervals. Movies of microtubule movements were compiled using Adobe Premier v6.0 software (Adobe Systems, Inc.). For immunolabeling of microtubule-MP complexes, chambers were constructed using poly-L-lysine-coated glass slides, and following the initiation of kinesin motor activity, chambers were perfused with 1% glutaraldehyde (in motility buffer) and incubated for 10 min at room temperature. Disassembled chambers were submerged for 10 min in 0.1% $NaBH_4$ (in phosphate-buffered saline), double labeled with antibodies against MP and α-tubulin (Oncogene Research Products), and visualized by fluorescence microscopy as described above.

RESULTS

MP confers resistance to microtubule-depolymerizing drugs in planta. It has been previously reported that TMV infection sites in *N. benthamiana* leaves continue to expand in the presence of microtubule-disrupting drugs (35, 51). In agreement, we found that a TMV strain carrying MP fused to mRFP1 (TMV-MP-mRFP1) could also spread following treatment of leaf tissue with oryzalin, colchicine, or amiprofos-methyl (APM). To characterize the distribution of MP in such treated leaves, TMV-MP-mRFP1 was used to infect transgenic *N. benthamiana* plants in which microtubules are labeled by a GFP fusion to *Arabidopsis* α-tubulin (*tua*-GFP) (35). Following the establishment of infection, leaves were infiltrated with 20 μM oryzalin, and the subcellular localization of MP-mRFP1 and *tua*-GFP was analyzed over a period of 90 min. Consistent with previous reports (35, 42, 81), we found that, prior to oryzalin infiltration, visible colocalization of MP-mRFP1 with microtubules was usually restricted to cells undergoing later stages of infection (Fig. 1A and B), whereas in cells at the front of infection, MP-mRFP1 predominantly accumulated at cell wall-proximal sites shown to correspond with Pd (data not shown) (79). Although *tua*-GFP-labeled microtubules were present in cells throughout the infection site both prior to oryzalin infiltration (Fig. 1C) and following mock-infiltration with water (Fig. 1D), no *tua*-GFP-labeled microtubules were observable in cells at the front of infection after treatment with oryzalin for 30 min (Fig. 1E and F). In contrast, a clear localization of MP-mRFP1 with intact *tua*-GFP-labeled microtubules could still be seen in cells behind the front of infection (Fig. 1G and H) after 30 min, although the prevalence of microtubule-associated MP was markedly reduced at 60 min posttreatment and thereafter. Thus, we could conclude from these data that, depending on the stage of TMV infection, microtubules could be protected against disruption by oryzalin in a manner corresponding to their association with MP-mRFP1.

MP stabilizes microtubules in BY-2 protoplasts. Next, we investigated whether the observed stabilization of microtubules can be attributed to the microtubule association of MP, as opposed to other MP or viral functions. Therefore, we infected BY-2 protoplasts with two different TMV derivatives expressing functional or nonfunctional MPs. At 24 h postinfection, the protoplasts were treated for 1 h with either 50 μM APM or 10 μM oryzalin, then immunolabeled with anti-α-tubulin antibody, and finally, analyzed by confocal microscopy.

In the absence of microtubule-disrupting agents, immunolabeled microtubules could be observed in both infected and healthy protoplasts (Fig. 2A), and as expected for protoplasts infected with TMV-MP-GFP, a clear colocalization of MP and microtubules could also be seen (Fig. 2A). In contrast to noninfected protoplasts, in which APM or oryzalin treatment led to a considerable reduction in the number of microtubules (Fig. 2B and C), infected protoplasts displayed a pattern of MP and microtubule labeling similar to that of untreated cells (Fig. 2B and C). Thus, TMV infection appeared to protect microtubules against disruption by APM and oryzalin.

To test whether the presence of virally encoded replicase proteins could be responsible for this observed microtubule protection, we infected protoplasts with a TMV derivative that replicates in protoplasts but expresses MP^{P81S}-GFP, a nonfunctional MP mutant which is diffusely distributed throughout the cytoplasm (Fig. 2D) (10). In contrast to results obtained using a virus encoding a functional MP, microtubules in protoplasts infected with TMV-MP^{P81S}-GFP were not similarly protected against APM and oryzalin treatment (Fig. 2E and F). Furthermore, in BY-2 cells bombarded with a plasmid encoding MP-yellow fluorescent protein under the control of the *Cauliflower Mosaic Virus* 35S promoter, expression of full-length MP outside a viral context was also sufficient to protect microtubules against drug-induced

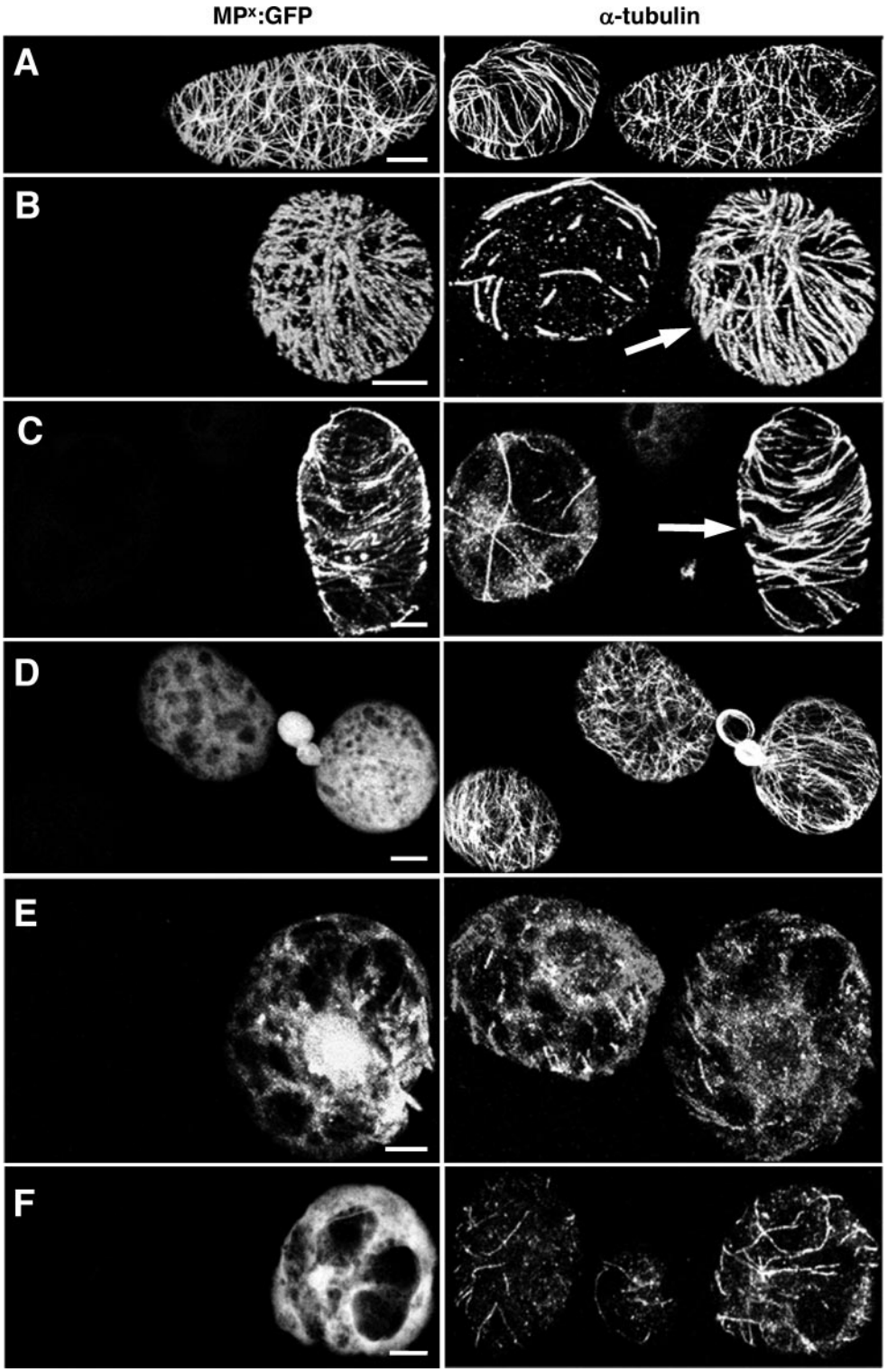

FIG. 2. MP stabilizes microtubules in BY-2 protoplasts. BY-2 protoplasts infected with TMV derivatives expressing functional or nonfunctional MPs were treated for 1 h with either 50 μM APM or 10 μM oryzalin and subsequently stained with anti-α-tubulin antibody. (A to C) BY-2 protoplasts infected with TMV-MP-GFP. (A) In the absence of microtubule-disrupting drugs, functional MP-GFP colocalizes with microtubules. (B and C) In nontransfected cells treated with APM (B) or oryzalin (C), microtubules are almost completely abolished. In cells infected with TMV-MP-GFP (arrows) treated under the same conditions, a high number of microtubules remain associated with MP-GFP. (D to F) BY-2 protoplasts infected with TMV-MP^{P81S}-GFP. (D) Nonfunctional MP^{P81S}-GFP is diffusely distributed throughout the cytoplasm in the absence of microtubule-disrupting drugs. (E and F) In nontransfected cells, treatment with APM (E) or oryzalin (F) leads to a dramatic disruption of microtubules. Under the same conditions, a similar loss of microtubules is apparent in cells expressing MP^{P81S}-GFP, indicating that the microtubule association of MP is required for microtubule stabilization against these drugs. Bar, 5 μm (A to D and F) and 10 μm (E).

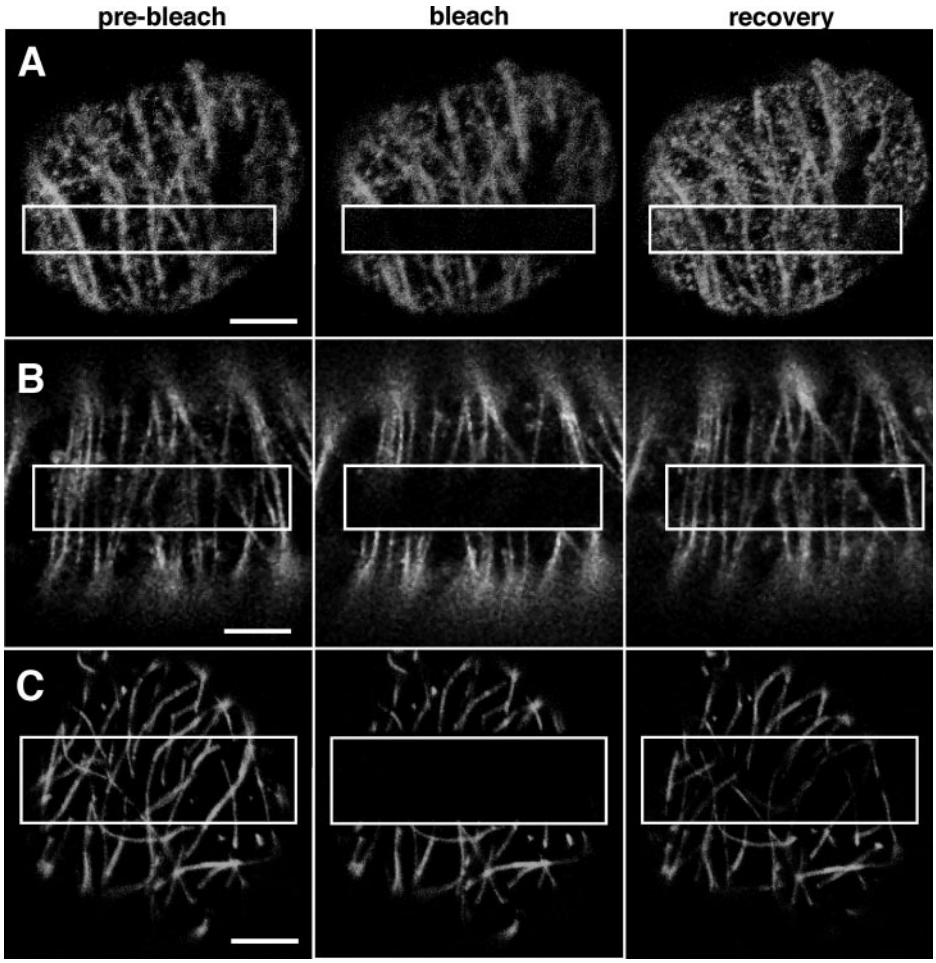

FIG. 3. FRAP of microtubule-associated MP-GFP and GFP–MAP65-5. (A) FRAP of microtubule-associated MP-GFP in BY-2 protoplasts infected with TMV-MP-GFP occurs uniformly within the bleached portion of the microtubules (box). MP-GFP does not visibly move from unbleached areas along the length of microtubules. (B) Microtubule-associated fluorescence recovers similarly in BY-2 cells ectopically expressing MP-GFP. (C) Characteristic of a structural MAP, GFP–MAP65-5 fluorescence recovers in a uniform manner within the bleached portion of microtubules. Bars, 5 μm.

disruption (data not shown). Therefore, these results clearly indicate that a functional MP capable of associating with microtubules is responsible for the in vivo protection of microtubules against disrupting drugs.

FRAP experiments demonstrate de novo recruitment of MP to microtubules. To address whether the association of MP with microtubules is the result of MP movement from its site of synthesis along the microtubule surface or de novo recruitment of MP from another compartment, we infected BY-2 protoplasts with TMV-MP-GFP and observed the FRAP of microtubule-aligned MP-GFP. At 18 h postinfection, FRAP of microtubule-associated MP-GFP first became evident about 3 min after bleaching and subsequently reached about 90% of the initial fluorescence level after 20 min (Fig. 3A). A similar level of FRAP was also observed after 20 min in transgenic BY-2 cells expressing MP-GFP from an inducible promoter out of viral context (Fig. 3B). Moreover, in both cases, recovery appeared to be uniform within the bleached area, that is, in no cases did MP-GFP appear to move directly along the microtubule from nonbleached areas into bleached areas. In parallel studies, the recovery of a GFP fusion to the *Arabidopsis* microtubule-associated protein MAP65-5 (99) was also investigated. Although FRAP of GFP–MAP65-5 only reached about 40 to 50% of the initial fluorescence after 20 min, the pattern of recovery was again uniform within the bleached area (Fig. 3C). Since the imaged microtubules may consist of microtubule bundles rather than individual microtubules, it might be possible that the apparent gradual recovery of MP-GFP fluorescence in the bleached region is due to a combined effect of MP-GFP movement along multiple microtubules in different directions. However, the similarity of MP-GFP recovery with the recovery of GFP–MAP65-5 rather suggests that MP is recruited to apparently nondynamic microtubules from a remote source and in a manner highly reminiscent of a typical MAP, such as *Arabidopsis* MAP65-5.

MP binds directly to dynamically suppressed microtubules in vitro. Although it has been previously reported that purified MP binds directly to tubulin in vitro (68), it remained unclear whether the MP was associated with true microtubules or tubulin dimers, since microtubules are known to exhibit a high

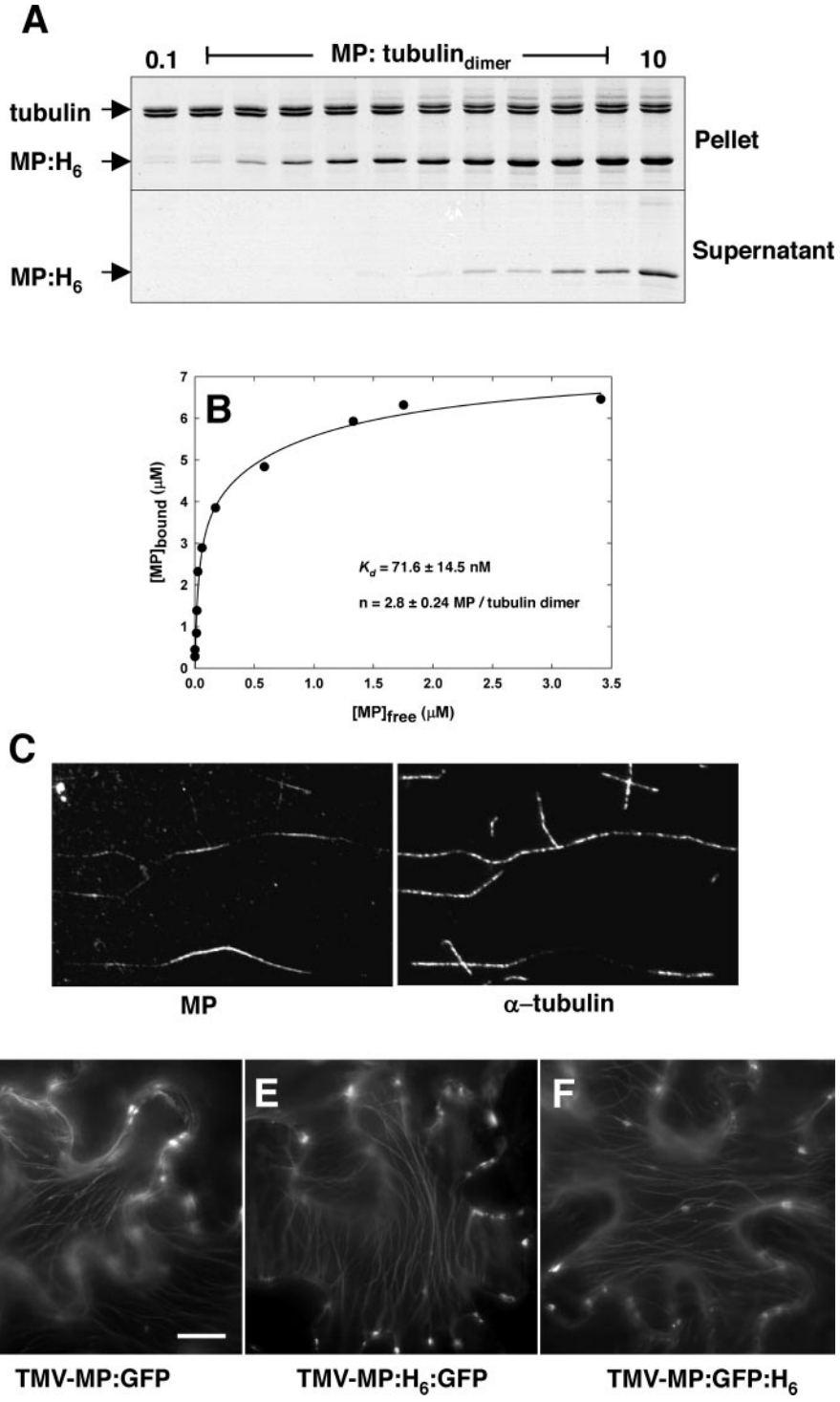

FIG. 4. MP binds saturably to dynamically stabilized microtubules in vitro. Paclitaxel-stabilized microtubules were polymerized in vitro and incubated with increasing amounts of MP-H_6. Microtubule-associated MP (Pellet) and unbound protein (Supernatant) were separated by centrifugation and analyzed by SDS-PAGE and Coomassie blue staining. (A) Saturation binding of purified MP-H_6 in the absence of microtubule polymerization dynamics. (B) Analysis of MP-microtubule binding parameters shows that MP binds microtubules with a relative affinity comparable to structural MAPs. (C) Fluorescence microscopy of the pellet fraction stained for MP and α-tubulin confirms that precipitated MP-H_6 is microtubule associated. (D to F) Polyhistidine does not effect the spread of TMV-MP-GFP and the subcellular distribution of MP-GFP during infection in *N. benthamiana* leaf epidermis. Bar, 10 μm.

degree of dynamic instability in vitro (7, 104). To test whether MP directly binds to microtubules in a manner similar to previously described MAPs or employs a novel coassembly mechanism (11), we utilized an in vitro sedimentation system in which purified MP in association with microtubules could be separated from unbound MP under conditions that strongly suppress microtubule dynamics. Briefly, MP was expressed in *E. coli* with a C-terminal His_6 tag fusion (MP-H_6) and purified

as previously described (10). Purified bovine brain tubulins were polymerized in vitro and dynamically stabilized by the addition of the antimitotic drug paclitaxel (29, 106). Increasing amounts of MP-H_6 were then incubated with 2.0 μM polymerized tubulin, and following sedimentation, pellet and supernatant fractions were analyzed by SDS-PAGE and colloidal Coomassie blue staining. As shown in Fig. 4A, tubulin is absent from the supernatant fractions, indicating that microtubules remained dynamically stable throughout the binding reaction. Moreover, the amount of MP-H_6 that cosedimented with microtubules remained constant at high MP concentrations, thus indicating that saturation binding of MP-H_6 to the surface of microtubules was not due to disordered MP aggregation.

In control experiments, no significant microtubule binding was observed when MP-H_6 was replaced by either BSA or GST-H_6 under the same conditions (data not shown). To verify that sedimenting MP-H_6 molecules are indeed bound to microtubules and do not precipitate because of self-aggregation, the pellet fractions were immunostained for MP and tubulin and subsequently analyzed by fluorescence microscopy. As shown in Fig. 4C, MP-H_6 was detected in association with microtubules, but significant amounts of nonspecific MP-H_6 aggregates were not observed. Similarly, in the absence of tubulin, MP-H_6 (up to 10 μM) remained almost exclusively (>95%) in supernatant fractions, as determined by scanning gel densitometry of colloidal Coomassie blue-stained SDS-PAGE gels (data not shown), thereby indicating that MP-H_6 preparations remained soluble.

To further test for a potential influence of the His_6 tag on the MP-microtubule interaction, TMV derivatives were constructed that expressed MP-GFP with a His_6 tag at either terminus of GFP (TMV-MP-H_6-GFP and TMV-MP-GFP-H_6). Upon infection of *N. benthamiana*, no difference in the subcellular localization of MP-H_6-GFP or MP-GFP-H_6 was observed compared to that previously reported for MP-GFP (42) (Fig. 4D to F). Collectively, these results indicate that the His_6 tag neither mediates the MP-microtubule interaction in vitro nor significantly affects the subcellular localization of MP-GFP in planta.

To further determine the binding parameters of the MP-microtubule interaction in vitro, the relative amount of MP-H_6 in the pellet and supernatant fractions was estimated by scanning gel densitometry of replicate gels. Values for $[MP]_{bound}$ were plotted versus $[MP]_{free}$, yielding a saturation hyperbole (Fig. 4B), and a curve was fit to these data using a noncatalytic bimolecular binding model (2). Nonlinear regression analysis of this curve gave an apparent K_D value of 71.6 ± 14.5 nM and binding stoichiometry of 2.8 ± 0.24 MP/$tubulin_{dimer}$. While it is unclear whether a single equivalent binding site for MP resides on the microtubule surface, or indeed, whether MP binds microtubules in a dimeric form (15), the estimated binding affinity of MP for microtubules is within the known range for high-affinity MAPs (2). We conclude from these data that, in the absence of dynamic tubulin polymerization or auxiliary factors, MP binds directly to the outer surface of microtubules with a relative affinity comparable to other MAPs.

MP-microtubule complexes are stable in vitro. Previously, it was shown that MP-associated microtubules isolated from infected BY-2 protoplasts were more resistant to disruption by high concentrations of NaCl or a combination of cold and calcium treatments (11). Since other cytoskeleton factors present in the extract may have contributed to the observed stability, we wished to determine whether a minimal MP-microtubule interaction would confer a similar effect. We therefore incubated paclitaxel-stabilized microtubules with recombinant MP-H_6 or recombinant H_6-*Tau* (MAP-to-tubulin molar ratio of 1:3) in reaction mixtures containing various amounts of NaCl and, as described above, analyzed the resulting complexes for microtubule-associated protein content. As expected for *Tau*, which associates with microtubules via predominantly ionic interactions (3, 20, 37, 46), treatment with NaCl concentrations of 0.3 M or greater led to a release of the protein from the microtubule surface (Fig. 5A). In contrast, MP remained attached to microtubules in a high ionic strength buffer (0.9 M NaCl), indicating that MP and *Tau* may interact with microtubules through nonequivalent binding sites (Fig. 5A). In another experiment, 3 μM paclitaxel-stabilized microtubules were incubated with increasing amounts of MP-H_6 prior to the addition of 10 mM $CaCl_2$ and subsequent incubation for 10

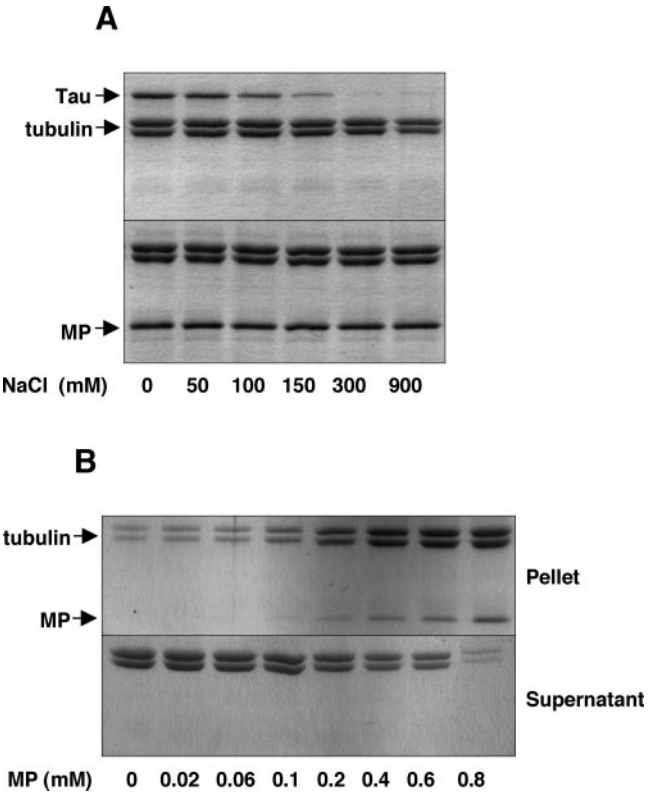

FIG. 5. MP-microtubule complexes are stable in vitro. Paclitaxel-stabilized microtubules were polymerized in vitro and incubated with MP-H_6 before being subjected to destabilizing conditions. Microtubule-associated MP and tubulin polymers (pellet) were separated from unbound protein and tubulin dimers (supernatant) by centrifugation and analyzed by SDS-PAGE and Coomassie blue staining. (A) In the presence of increasing concentrations of NaCl (>100 mM), purified *Tau* protein is released from the surface of purified microtubules polymerized in vitro (upper panel). Under the same reaction conditions, purified MP-H_6 remains bound to microtubules at NaCl concentrations of up to 0.9 M (bottom panel). (B) Prior incubation of in vitro-polymerized microtubules with submolar amounts of MP-H_6 protects microtubules against strongly destabilizing conditions (10 mM $CaCl_2$ at 4°C).

min at 4°C. As shown in Fig. 5B, such conditions were sufficient to strongly destabilize microtubules in vitro in the absence of MP; however, at an approximate MP-to-tubulin molar ratio of 1:3, over 90% of the tubulin remained in the pellet fraction, thus indicating that, in the absence of auxiliary plant or viral factors, MP can enhance microtubule stability by directly binding the microtubule surface in a salt stable manner.

Microtubules do not mediate the degradation of ubiquitinated MP. TMV MP is believed to be targeted for degradation by the ubiquitin/26S proteasome (Ub/26S) pathway (85). Furthermore, it has been speculated that microtubules may be involved in Ub/26S targeting of MP (35, 66, 85), implying that microtubule-associated MP is a substrate for ubiquitination. To test this possibility, we isolated cytoskeleton-enriched fractions from BY-2 protoplasts infected with three different TMV derivatives and subsequently analyzed their protein content by SDS-PAGE and immunolabeling with antibodies against ubiquitin and MP, respectively. As a control for possible contamination by replication body proteins, we infected protoplasts with TMV-MP-GFP, which expresses wild-type MP that associates with Pd as well as with both microtubules and large inclusion bodies (Fig. 6A). In addition, we also infected protoplasts with a TMV derivative expressing $MP^{\Delta C55}$-GFP, which almost exclusively associates with microtubules and Pd (Fig. 6D) (13), and a derivative expressing MP^{P81S}-GFP, which localizes to Pd in planta and is dispersed in the cytoplasm of BY-2 protoplasts (Fig. 6G) (10).

Analysis of crude protein extracts from protoplasts infected with TMV-MP-GFP showed that MP-GFP was present at both the expected 62-kDa mass and also as higher-molecular-mass forms (Fig. 6, lane 8). The appearance of the high-molecular-weight MP moieties is consistent with the pattern of ubiquitinated proteins found in the same extract (Fig. 6J, lane 4) and indicates that a fraction of the MP had been subjected to ubiquitination. The MP found in the cytoskeleton-enriched fractions, however, appeared to migrate exclusively at the expected size for monomeric MP-GFP fusion proteins (Fig. 6J, lanes 5 and 6). While polyubiquitinated proteins were detected in these fractions (Fig. 6J, lanes 1 and 2) as well as in the MP-deficient cytoskeletal fraction of cells infected with TMV-MP^{P81S}-GFP (Fig. 6J, lanes 3 and 7), the sets of MP-specific and ubiquitin-specific bands did not overlap, thereby indicating that microtubule-associated MP was not ubiquitinated.

To further determine whether microtubules were involved in the degradation of MP in planta, transgenic *N. benthamiana* plants expressing *tua*-GFP were infected with TMV-MP-GFP, and leaf disks containing initial small infection sites were infiltrated with water or 50 μM APM. Subsequently, the growing infection sites were analyzed by microscopy over a period of 5 days. In infection sites of mock-infiltrated leaf disks, MP-GFP was present in cytoplasmic and cell wall-proximal inclusions, and *tua*-GFP- or MP-GFP-labeled microtubules could be observed throughout the infection site (Fig. 6K). In contrast, observable *tua*-GFP-labeled and MP-GFP-labeled microtubules were absent in cells of infection sites grown in tissue treated with APM, although in both nontransgenic *N. benthamiana* (not shown) and plants expressing *tua*-GFP (Fig. 6N), cell wall-localized aggregates of MP-GFP were apparent in cells corresponding to early and mid stages of infection. In agreement with previous reports (35), ongoing cell-to-cell movement of TMV-MP-GFP in both mock- and APM-infiltrated tissues was characterized by the continued radial expansion of fluorescent, ring-shaped infection sites (Fig. 6L, M, O, and P), yet in contrast to Gillespie et al. (35), we observed that, in the absence of an effect of APM treatment on MP-GFP expression levels (Fig. 6Q), the expansion rate of infection sites in APM-treated tissues was clearly reduced compared to the respective rate in mock-treated tissues (Fig. 6R). Moreover, although the subcellular distribution of MP-GFP was dramatically altered in APM-treated tissue, the expanding infection sites retained a characteristic dark inner disk (Fig. 6P) corresponding to the absence of MP-GFP fluorescence at very late stages of infection. Therefore, assuming that the apparent absence of MP-GFP from the center of infection sites is representative of Ub/26S-dependent degradation of MP, as previously proposed (85), the observation that MP-GFP in APM-treated leaf had been degraded to levels comparable with mock-infiltrated tissue (Fig. 6M) supports the conclusion that microtubules are not directly involved in the turnover of MP during TMV infection and that microtubule-associated MP does not represent the Ub/26S degradation pathway.

Effects of MP MAP activity on molecular motor transport. Although organelle trafficking is believed to be largely actin dependent in plants (8, 14, 25, 90), we speculated that, since MP associates with actin microfilaments (68), microtubules, and abnormal ER-derived aggregates (6, 42, 51, 86), the accumulation of MP on microtubules might be inhibitory to actin-dependent transport or the formation and movement of membranous organelles, such as Golgi. Therefore, we cobombarded BY-2 cells with constructs expressing mRFP fused to α-1,2 mannosidase-1, a *cis*-Golgi resident protein (Man-1–mRFP) (74), and $MP^{\Delta C55}$-GFP5, an MP deletion mutant which predominantly associates with microtubules (13).

Analysis of transfected cells by confocal microscopy revealed that while $MP^{\Delta C55}$-GFP5 clearly accumulated on microtubules (Fig. 7A), a significant number of motile Man-1-labeled Golgi stacks were apparent (Fig. 7B to D). The majority of observed Golgi stacks displayed saltatory motions and typically traveled for short distances (approximately 0.5 to 2 μm) before intermittently stalling or changing direction. Of those that appeared to travel along relatively linear trajectories, the average movement velocity was estimated to be 0.095 ± 0.031 mm/s ($n = 32$ movement events), consistent with previous reports of Golgi streaming in BY-2 culture cells (74). Although it is still unclear whether the temporal effects of MP on ER morphology or the association of MP with actin would modulate Golgi movements in planta, these data suggest that the accumulation of MP on microtubules is not inhibitory to actinomyosin-based transport.

Since it has been shown that microtubule association of MAP2 and *Tau* proteins are inhibitory to molecular motor activity, both in vivo (31, 95, 98) and in vitro (38, 63, 93, 102), we speculated that the interaction of MP with microtubules might have a similar effect. To test this hypothesis, rhodamine-labeled microtubules were absorbed onto the surface of a glass perfusion chamber precoated with human kinesin 1. Following the addition of purified MP-H_6 or control proteins, the chambers were rinsed and microtubule translocations were recorded by digital fluorescence microscopy. In agreement with previous reports (93), the average kinesin-dependent microtubule trans-

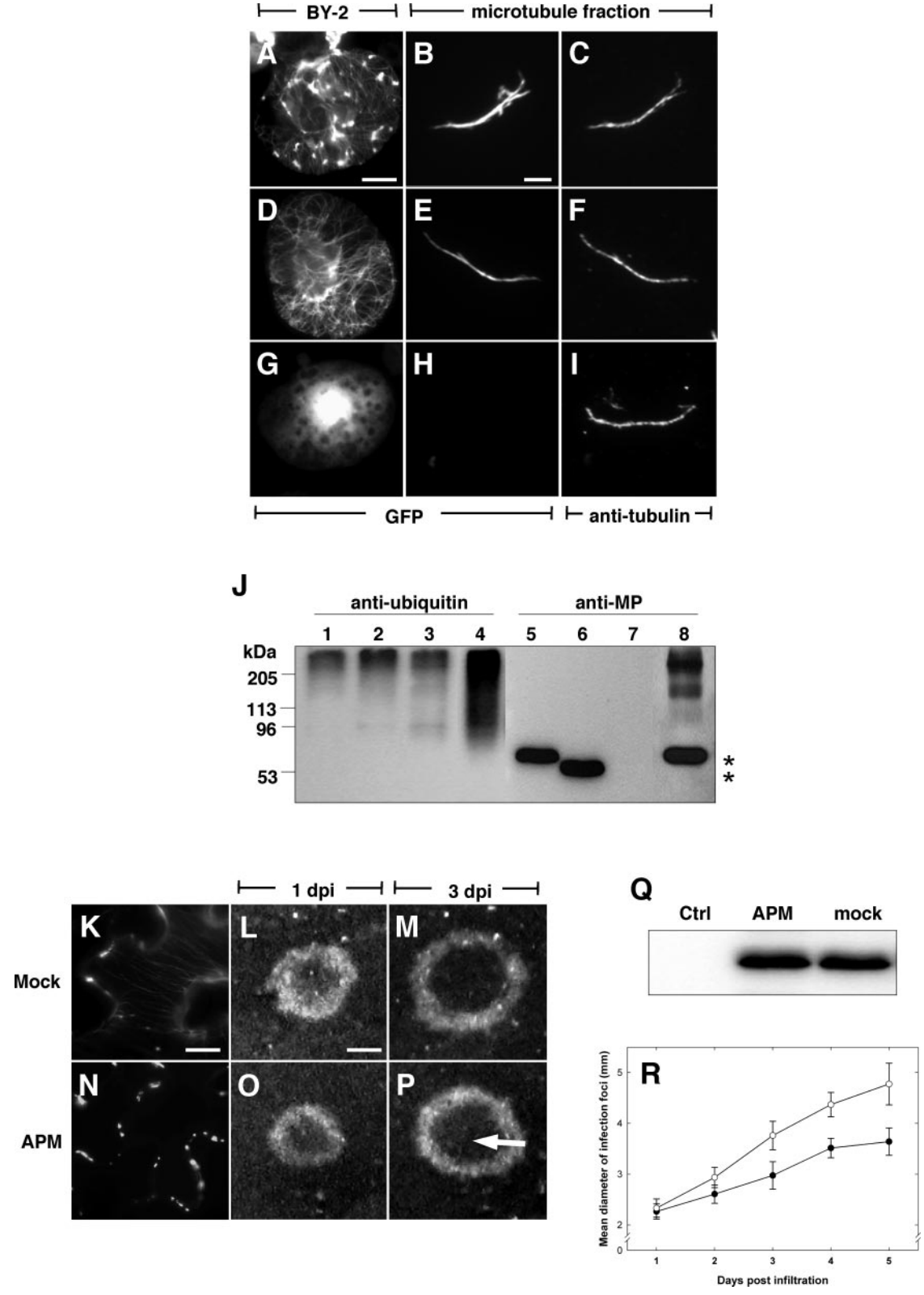

FIG. 6. Microtubules do not mediate the degradation of ubiquitinated MP. Cytoskeleton-enriched fractions isolated from BY-2 protoplasts infected with TMV-MP-GFP (A to C and J, lanes 1 and 5), TMV-MP$^{\Delta C55}$-GFP (D to F and J, lanes 2 and 6), and TMV-MP^{P81S}-GFP (G to I and J, lanes 3 and 7) were analyzed by Western blotting with antibodies against ubiquitin (J, lanes 1 to 4) and MP (J, lanes 5 to 8), respectively. In contrast to MP-GFP in crude extracts from TMV-MP-GFP-infected cells (J, lanes 4 and 8), microtubule-associated MP-GFP migrates exclusively at the expected molecular mass for monomeric proteins (*) (J, lanes 5 and 6) and does not cross-react with anti-ubiquitin (J, lanes 1 and 2). (K to P) TMV-MP-GFP infection in leaf disks from *tua*-GFP transgenic *N. benthamiana* following infiltration with water (K to M) or 50 μM APM

location rate was found to be 0.20 ± 0.052 μm/s in the absence of MP-H_6 (Fig. 7E). Because only a small proportion of the microtubules actually absorbed to the chamber surface (not shown), we were unable to accurately determine the final tubulin concentration. Nevertheless, when MP-H_6 was present at levels expected to saturate the estimated binding stoichiometry of 1.4 MP per tubulin monomer (Fig. 7H and I), kinesin-dependent microtubule movements were almost completely abolished (Fig. 7F).

In control experiments, equivalent amounts of MP-H_6 (1 μM) were added to the perfusion chamber prior to introducing the fluorescent microtubules. Since microtubules appeared to smoothly glide across the chamber surface under these conditions (not shown), we conclude that MP-H_6 did not directly bind kinesin or nonspecifically anchor microtubules to the glass surface. To further control for possible nonspecific inhibition of kinesin motor activity, MP-H_6 was replaced by GST-H_6 (1 μM), a protein previously shown not to bind microtubules in vitro (not shown). While the presence of GST-H_6 led to a slight decrease in the average kinesin-dependent translocation rate (0.14 ± 0.058 μm/s), microtubule movements were largely unaffected (Fig. 7G), thus indicating that the observed kinesin inhibition was due to a particular property of MP.

To determine whether MP-H_6 was indeed present on the surface of the microtubules, protein complexes within the chamber were chemically fixed 20 min after MP-H_6 was introduced and subsequently stained with antibodies against MP and tubulin. Consistent with the in vitro binding experiments and previous in vivo data, MP-H_6 was clearly associated with the microtubules along their entire length (Fig. 7H and I). Although further experiments using low amounts of kinesin at known MP/tubulin ratios will be required to determine whether MP inhibits kinesin translocation in a manner similar to other MAPs (63, 93), the above data nevertheless support the idea that, during late infection, the accumulation of MP on microtubules could negatively regulate microtubule-dependent trafficking of endogenous plant and/or viral factors.

DISCUSSION

As the name suggests, MAPs are simply defined as proteins that directly interact with the surface of microtubules. Thus, the uniform distribution of MP-GFP along microtubules observed during late infection is generally consistent with the microtubule localization of plant MAPs (61, 62, 94, 99, 105). Unlike processive molecular motors, which can translocate along the length of microtubules, FRAP experiments indicated that irrespective of viral infection, fluorescence attributable to MP-GFP in unbleached microtubule areas does not move longitudinally into bleached areas. Thus, under our experimental conditions, the microtubule-associating properties of MP seem to be inconsistent with that of a motor protein. Moreover, these data suggest that deployment of MP to the microtubule surface is unlikely to occur by means of a motile motor protein at late stages of infection, in which microtubules are heavily decorated with MP. Due to limits of microscope resolution, we were unable to determine the exact source of the unbleached MP-GFP. However, MP is characteristic of an integral membrane protein (16, 86), and single-point mutations within the predicted transmembrane domain of MP render the protein unable to associate with microtubules or facilitate cell-to-cell movement of TMV at nonpermissive temperature (11). While the exact nature of the mutant MP dysfunction remains unknown, the fact that microtubule association is inhibited may suggest that endomembranes are involved in the deployment of MP to microtubules. On the other hand, since our in vitro experiments clearly demonstrate that MP can directly interact with the surface of dynamically stabilized microtubules, a prior association of MP with endomembranes seems not to be a prerequisite for microtubule association. Given that MP binds microtubules with a relative affinity comparable to other MAPs, the fluorescence recovery of MP-GFP is similar to that of GFP-MAP65-5, and MP interacts with the prokaryotic tubulin homologue FtsZ (43) and microtubules in various systems (11), we conclude that MP has a functionally conserved affinity for microtubules and behaves in a manner consistent with a structural MAP.

The above data imply that MP does not incorporate into the microtubule lattice by the previously suggested mechanism of dynamic coassembly (11); however, it is clear that the MAP activity of MP confers resistance against microtubule-disrupting conditions upon ectopic expression in BY-2 cells, during infection of plants and in vitro. Recently, it was determined that MP stabilizes microtubules also upon expression in mammalian cells (33). Modulation of microtubule dynamic instability is a common feature of structural MAPs (83, 91, 100) and is thought to involve the reduction of interdimer charge-repulsion forces due to binding of MAPs to the microtubule surface (3, 20). Thus, it is not surprising that MP-dependent protection against microtubule-disrupting drugs is apparent in cells containing microtubules heavily decorated with MP-GFP. Based on previous studies, it is unclear whether microtubule association is strictly dependent on MP expression level (12); however, because oryzalin is thought to bind tubulin dimers and destabilize interprotofilament contacts during microtubule polymerization (48, 71, 73), our results in fact suggest that MP reduces the turnover of microtubules that had polymerized

(N to P). In mock-infiltrated cells behind the infection front, MP-GFP localizes to microtubules and cell wall inclusions (K). In contrast, *tua*-GFP-labeled and MP-GFP-labeled microtubules are absent throughout the infection site up to 5 days following APM treatment; however, MP-GFP remains localized to cell wall inclusions (N). Infection sites continue to expand radially following mock (L and M) or APM (O and P) infiltration, and in both cases, a normal level of MP-GFP turnover is characterized by the absence of MP-GFP fluorescence within the center of the infection site (P, arrow). (Q) Western blot of relative MP-GFP abundance in mock-treated and APM-treated TMV-MP-GFP infection sites at 5 days postinfiltration. (R) Growth rates of TMV-MP-GFP infection sites in leaves infiltrated with APM (black circles) or water (white circles). Error bars in panel R correspond to 95% confidence intervals. Bars, 5 μm (A, D, and G); 3 μm (B, C, E, F, H, and I); 10 μm (K and N); and 1 mm (L, M, O, and P).

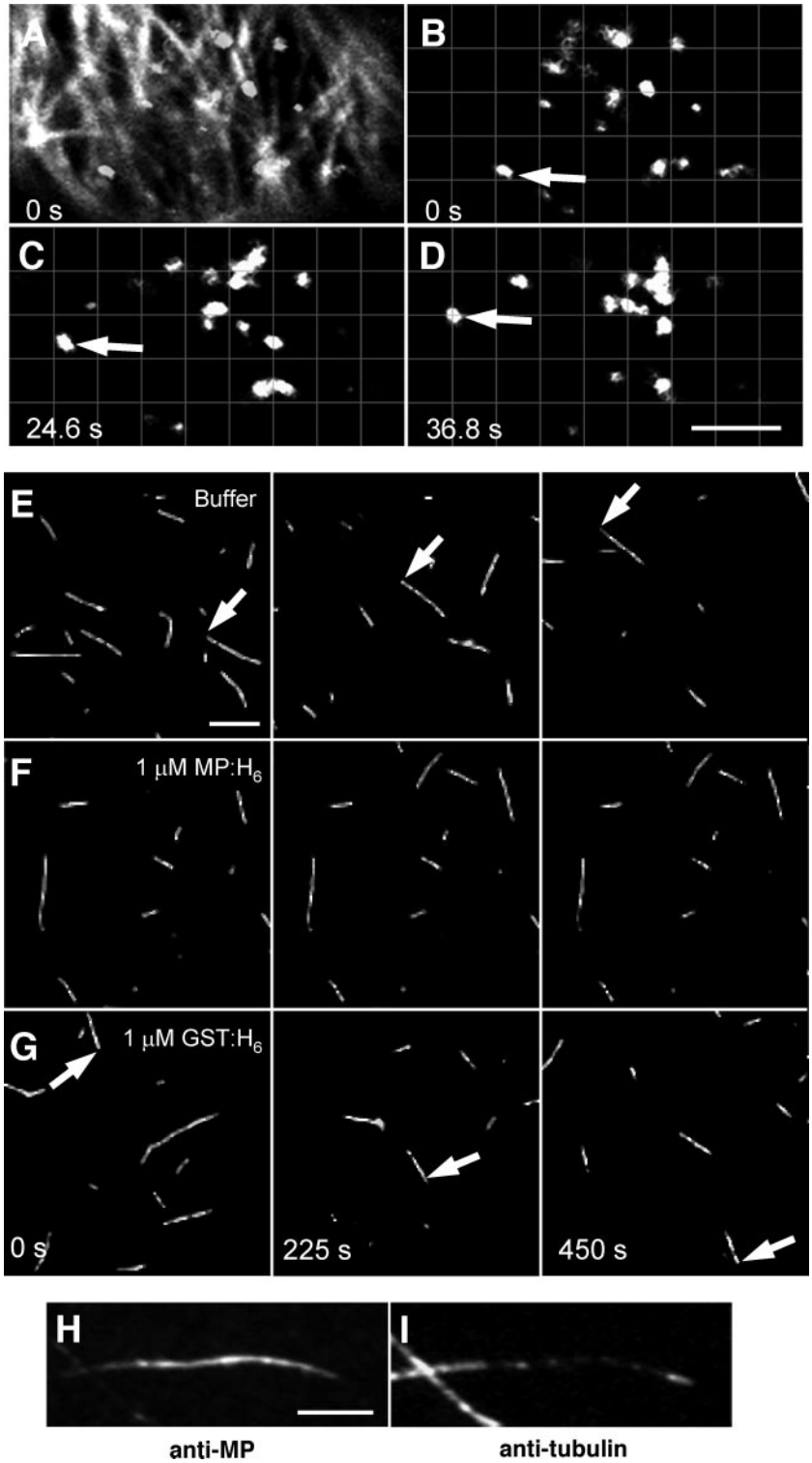

FIG. 7. Effects of MP MAP activity on molecular motor transport. (A to D) The microtubule association of MP does not inhibit Golgi stack movements in BY-2 cells infected with TMV-$MP^{\Delta C55}$-GFP or ectopically expressing $MP^{\Delta C55}$-GFP. In cells where $MP^{\Delta C55}$-GFP is clearly associated with microtubules (panel A, overlay of the $MP^{\Delta C55}$-GFP signal [filaments] and Man-1-mRFP signal [bodies, i.e., Golgi complexes], compare with panel B), movements of Man-1-mRFP-labeled Golgi stacks (B to D) are apparent at an average velocity of 0.095 ± 0.031 μm/s. Bar, 4 μm. (E to G) Time-lapse recordings of fluorescent microtubules translocating along the surface of a perfusion chamber coated with kinesin-1. Bar, 4 μm. (E) In the absence of exogenous proteins, microtubules translocate at an average velocity of 0.2 ± 0.052 μm/s. (F) The presence of 1 μM MP-H_6 completely abolishes kinesin-dependent microtubule translocation. (G) Kinesin-dependent microtubule movements are still apparent in the presence of 1 mM GST-H_6 at an average velocity of 0.14 ± 0.058 μm/s. (H and I) Microtubules immobilized within kinesin-coated perfusion chambers are highly decorated in the presence of 1 μM MP-H_6. Bar, 1.5 μm.

prior to oryzalin reaching inhibitory concentrations. Although understanding the structural basis of MP-dependent microtubule stabilization requires further studies, resistance of the MP-microtubule interaction to high ionic strength indicates a hydrophobic and/or high-affinity component to the binding mechanism, a fact reflected in the ability of MP to decorate microtubules in the presence of other plant MAPs and to counteract the effects of microtubule-destabilizing conditions.

The function of MP-associated microtubules remains unknown. Since their occurrence late in infection is correlated with the movement function of MP during early infection, these complexes may just reflect a previous microtubule-based event, without themselves having a specific function during late infection (12). In fact, similar to previous reports (35, 51), we found that the apparent disruption of microtubules by treatment of infection sites with APM did not abolish further spread of TMV infection. However, drug treatments do not result in the complete disruption of all microtubules throughout the infiltrated tissue (92), and given that viral replication complexes have been observed in close proximity to Pd (32, 81), it is conceivable that incomplete disruption of microtubules would be sufficient to permit limited tubulin-based movement in the vicinity of Pd (92). However, while limited viral spread may still persist after drug treatment, the apparent absence of detectable MP-associated microtubules in treated tissues indicates that the MAP activity of MP late in infection is not essential for the cell-to-cell movement of TMV infection in *N. benthamiana*. Interestingly, radial expansion of TMV-MP-GFP infection sites was approximately 25% slower in APM-treated tissue than in mock-infiltrated leaves (Fig. 6), suggesting that the MAP activity of MP may serve a specialized secondary role to support efficient infection. Since MP is ubiquitinated in tobacco protoplasts (85) and associates with microtubules prior to its degradation at late stages of infection (66, 86), it has been suggested that targeting of MP for degradation by the 26S proteasome is microtubule dependent (35). Here, we tested this possibility and found that, although polyubiquitinated MP was present in crude extracts from protoplasts infected with TMV derivatives, corresponding high-molecular-weight forms of MP were absent from cytoskeleton-enriched fractions, indicating that the association of MP with microtubules is unlikely to represent the ubiquitin-mediated degradation pathway for MP. It was previously reported that specific proteasome inhibitors led to increased levels of stable, high-molecular-weight forms of MP in protoplasts (85) and the apparent redistribution of MP from microtubules onto cortical ER in planta (35). Given that stable polyubiquitinated proteins are likely to accumulate in the proteasome-targeting pathway under these conditions and that a precedent exists for an ER-associated degradation system in plants (52, 72), it appears likely that, independent of microtubules, ER mediates the proteasome-dependent degradation of MP. Moreover, the aforementioned FRAP and in vitro experiments suggest that MP is only transiently present on the microtubule surface, and since MP is characteristic of an integral membrane protein, it remains probable that MP has the capacity to enter an ER-associated degradation targeting pathway independent of its prior association with microtubules.

The observation that microtubule association of MP leads to severe inhibition of kinesin motor function in vitro suggests that MP-associated microtubules are not only stabilized but also defective for motor-mediated transport. Based on this observation, we propose that MP-associated microtubules may block microtubule-based transport activities during late infection. Unfortunately, due to the lack of an appropriate experimental system in leaf epidermis, we were not able to test whether such inhibition indeed occurs in vivo or is beneficial to the TMV infection strategy. The fact that MP-transgenic plants are phenotypically identical to wild-type plants (27) may argue against this possibility, given that microtubule-motor proteins are required for cytokinesis (4, 59, 75, 97). However, it should be noted that transgenic MP has not been observed to associate with microtubules in such plants and, therefore, seems not to reflect the behavior of virally expressed MP with regard to microtubule association during late infection.

The finding that reduced movement efficiency in APM-treated tissues is correlated with the association of MP-GFP with aberrant cell wall-proximal aggregates further suggests the possibility that microtubules and associated motor activities are involved in the proper coordination of viral activities and localization of MP. One could envisage that microtubules might serve as a conduit for the effective sequestration of excess MP, which in turn, could circumvent the obstruction of Pd by limiting the availability of MP for entry into the Pd trafficking pathway. An alternative proposal is that microtubule-associated MP is involved in the down-regulation of viral replication and of subsequent pathogenesis at late stages of infection. This could be achieved by inhibiting the deployment of host factors involved in TMV translation, such as the microtubule-associated, kinesin-like translation enhancer eIF4(iso)F (9, 34), or by the concomitant sequestration of replication components to microtubules (66, 67) and recovery of ER to a preinfection morphology (86). Although the MP has an inherent binding affinity for microtubules, as determined by transient expression in plant and animal cells (11, 33, 42, 86) and also as shown by in vitro experiments described herein, the MP also accumulates at other cellular sites during infection (42), indicating that the microtubule-binding functions of MP are regulated in infected cells. Recently, an MP-binding protein termed MBP2C has been implicated in having a role in the accumulation of MP on microtubules (58). Thus, although MP has the capacity to bind microtubules in vitro in the absence of other auxiliary factors, the microtubule-binding activity might be tightly controlled during infection in vivo, e.g., through association of MP with cellular membranes or with other proteins. Although preliminary data indicate that a potentially nontranslatable (50) MP-vRNA-microtubule ribonucleoprotein complex can be reconstituted in vitro (data not shown), further studies will be required to fully elucidate the roles of microtubules and MP in the cell-to-cell movement process of TMV.

ACKNOWLEDGMENTS

We thank D. Geelen (Department of Plant Systems Biology, Gent University, Belgium) for GFP–MAP65-5 and *tua*-GFP constructs, R. Tsien (Department of Chemistry and Biochemistry, UCSD) for mRFP1, H. Vogler and V. Boyko for the pGII-Ω-35SHA construct, A. Karsies-Van Eeden for pTA-MP:GFP, C. Fitterer for pBP30-GmMan1:RFP bombardments as well as for support in the immunostaining experiments, and K. Oparka for providing seeds of *N.*

benthamiana transgenic for *tua*-GFP. We also thank K. Oparka for allowing us to have access to unpublished data from his laboratory.

This work was supported by the Novartis Research Foundation, the Swiss National Science Foundation (grant 631-65953.01), and the French Centre National de la Recherche Scientifique (CNRS). A.S. received support from the Ciudad Valenciana (Spain).

REFERENCES

1. **Aaziz, R., S. Dinant, and B. L. Epel.** 2001. Plasmodesmata and plant cytoskeleton. Trends Plant Sci. **6:**326–330.
2. **Ackmann, M., H. Wiech, and E. Mandelkow.** 2000. Nonsaturable binding indicates clustering of tau on the microtubule surface in a paired helical filament-like conformation. J. Biol. Chem. **275:**30335–30343.
3. **Al-Bassam, J., R. S. Ozer, D. Safer, S. Halpain, and R. A. Milligan.** 2002. MAP2 and tau bind longitudinally along the outer ridges of microtubule protofilaments. J. Cell Biol. **157:**1187–1196.
4. **Ambrose, J. C., W. Li, A. Marcus, H. Ma, and R. Cyr.** 2005. A minus-end-directed kinesin with plus-end tracking protein activity is involved in spindle morphogenesis. Mol. Biol. Cell **16:**1584–1592.
5. **Aoyama, T., and N. H. Chua.** 1997. A glucocorticoid-mediated transcriptional induction system in transgenic plants. Plant J. **11:**605–612.
6. **Asurmendi, S., R. H. Berg, J. C. Koo, and R. N. Beachy.** 2004. Coat protein regulates formation of replication complexes during tobacco mosaic virus infection. Proc. Natl. Acad. Sci. USA **101:**1415–1420.
7. **Billger, M. A., G. Bhattacharjee, R. C. Williams, Jr., and G. Bhatacharjee.** 1996. Dynamic instability of microtubules assembled from microtubule-associated protein-free tubulin: neither variability of growth and shortening rates nor "rescue" requires microtubule-associated proteins. Biochemistry **35:**13656–13663.
8. **Boevink, P., K. Oparka, S. Santa Cruz, B. Martin, A. Betteridge, and C. Hawes.** 1998. Stacks on tracks: the plant Golgi apparatus traffics on an actin/ER network. Plant J. **15:**441–447.
9. **Bokros, C. L., J. D. Hugdahl, H. H. Kim, V. R. Hanesworth, A. van Heerden, K. S. Browning, and L. C. Morejohn.** 1995. Function of the p86 subunit of eukaryotic initiation factor (iso)4F as a microtubule-associated protein in plant cells. Proc. Natl. Acad. Sci. USA **92:**7120–7124.
10. **Boyko, V., J. A. Ashby, E. Suslova, J. Ferralli, O. Sterthaus, C. M. Deom, and M. Heinlein.** 2002. Intramolecular complementing mutations in *Tobacco mosaic virus* movement protein confirm a role for microtubule association in viral RNA transport. J. Virol. **76:**3974–3980.
11. **Boyko, V., J. Ferralli, J. Ashby, P. Schellenbaum, and M. Heinlein.** 2000. Function of microtubules in intercellular transport of plant virus RNA. Nat. Cell Biol. **2:**826–832.
12. **Boyko, V., J. Ferralli, and M. Heinlein.** 2000. Cell-to-cell movement of TMV RNA is temperature-dependent and corresponds to the association of movement protein with microtubules. Plant J. **22:**315–325.
13. **Boyko, V., J. van der Laak, J. Ferralli, E. Suslova, M.-O. Kwon, and M. Heinlein.** 2000. Cellular targets of functional and dysfunctional mutants of tobacco mosaic virus movement protein fused to GFP. J. Virol. **74:**11339–11346.
14. **Brandizzi, F., C. Saint-Jore, I. Moore, and C. Hawes.** 2003. The relationship between endomembranes and the plant cytoskeleton. Cell Biol. Int. **27:**177–179.
15. **Brill, L. M., S. Dechongkit, B. DeLaBarre, J. Stroebel, R. N. Beachy, and M. Yeager.** 2004. Dimerization of recombinant tobacco mosaic virus movement protein. J. Virol. **78:**3372–3377.
16. **Brill, L. M., R. S. Nunn, T. W. Kahn, M. Yeager, and R. N. Beachy.** 2000. Recombinant tobacco mosaic virus movement protein is an RNA-binding, alpha-helical membrane protein. Proc. Natl. Acad. Sci. USA **97:**7112–7117.
17. **Cai, G., S. Romagnoli, A. Moscatelli, E. Ovidi, G. Gambellini, A. Tiezzi, and M. Cresti.** 2000. Identification and characterization of a novel microtubule-based motor associated with membranous organelles in tobacco pollen tubes. Plant Cell **12:**1719–1736.
18. **Campbell, R. E., O. Tour, A. E. Palmer, P. A. Steinbach, G. S. Baird, D. A. Zacharias, and R. Y. Tsien.** 2002. A monomeric red fluorescent protein. Proc. Natl. Acad. Sci. USA **99:**7877–7882.
19. **Carrington, J. C., K. D. Kasschau, S. K. Mahajan, and M. C. Schaad.** 1996. Cell-to-cell and long distance transport of viruses in plants. Plant Cell **8:**1669–1681.
20. **Cassimeris, L., and C. Spittle.** 2001. Regulation of microtubule-associated proteins. Int. Rev. Cytol. **210:**163–226.
21. **Chan, J., T. Rutten, and C. Lloyd.** 1996. Isolation of microtubule-associated proteins from carrot cytoskeletons: a 120 kDa map decorates all four microtubule arrays and the nucleus. Plant J. **10:**251–259.
22. **Citovsky, V., D. Knorr, G. Schuster, and P. Zambryski.** 1990. The P30 movement protein of tobacco mosaic virus is a single-stranded nucleic acid binding protein. Cell **60:**637–647.
23. **Citovsky, V., M. L. Wong, A. L. Shaw, B. V. Venkataram Prasad, and P. Zambryski.** 1992. Visualization and characterization of tobacco mosaic virus movement protein binding to single-stranded nucleic acids. Plant Cell **4:**397–411.
24. **Criqui, M. C., Y. Parmentier, A. Derevier, W. H. Shen, A. Dong, and P. Genschik.** 2000. Cell cycle-dependent proteolysis and ectopic overexpression of cyclin B1 in tobacco BY2 cells. Plant J. **24:**763–773.
25. **daSilva, L. L., E. L. Snapp, J. Denecke, J. Lippincott-Schwartz, C. Hawes, and F. Brandizzi.** 2004. Endoplasmic reticulum export sites and Golgi bodies behave as single mobile secretory units in plant cells. Plant Cell **16:**1753–1771.
26. **Dawson, W. O., P. Bubrick, and G. L. Grantham.** 1988. Modifications of the tobacco mosaic virus coat protein gene affecting replication, movement, and symptomatology. Phytopathology **78:**783–789.
27. **Deom, C. M., K. R. Schubert, S. Wolf, C. A. Holt, W. J. Lucas, and R. N. Beachy.** 1990. Molecular characterization and biological function of the movement protein of tobacco mosaic virus in transgenic plants. Proc. Natl. Acad. Sci. USA **87:**3284–3288.
28. **Deom, C. M., M. Lapidot, and R. N. Beachy.** 1992. Plant virus movement proteins. Cell **69:**221–224.
29. **Derry, W. B., L. Wilson, and M. A. Jordan.** 1995. Substoichiometric binding of taxol suppresses microtubule dynamics. Biochemistry **34:**2203–2211.
30. **Ding, B., J. S. Haudenshield, R. J. Hull, S. Wolf, R. N. Beachy, and W. J. Lucas.** 1992. Secondary plasmodesmata are specific sites of localization of the tobacco mosaic virus movement protein in transgenic tobacco plants. Plant Cell **4:**915–928.
31. **Ebneth, A., R. Godemann, K. Stamer, S. Illenberger, B. Trinczek, and E. Mandelkow.** 1998. Overexpression of tau protein inhibits kinesin-dependent trafficking of vesicles, mitochondria, and endoplasmic reticulum: implications for Alzheimer's disease. J. Cell Biol. **143:**777–794.
32. **Epel, B. L., H. S. Padgett, M. Heinlein, and R. N. Beachy.** 1996. Plant virus movement protein dynamics probed with a GFP-protein fusion. Gene **173:**75–79.
33. **Ferralli, J., J. Ashby, M. Fasler, V. Boyko, and M. Heinlein.** 2006. Disruption of microtubule organization and centrosome function by expression of *Tobacco mosaic virus* movement protein. J. Virol. **80:**5807–5821.
34. **Gallie, D. R.** 2002. The 5′-leader of tobacco mosaic virus promotes translation through enhanced recruitment of eIF4F. Nucleic Acids Res. **30:**3401–3411.
35. **Gillespie, T., P. Boevink, S. Haupt, A. G. Roberts, R. Toth, T. Vantine, S. Chapman, and K. J. Oparka.** 2002. Functional analysis of a DNA shuffled movement protein reveals that microtubules are dispensable for the cell-to-cell movement of tobacco mosaic virus. Plant Cell **14:**1207–1222.
36. **Grolig, F.** 2004. Organelle movements: transport and positioning, p. 148–175. *In* P. J. Hussey (ed.), The plant cytoskeleton in cell differentiation and development, vol. 10. Blackwell Publishing, Oxford, United Kingdom.
37. **Gustke, N., B. Trinczek, J. Biernat, E. M. Mandelkow, and E. Mandelkow.** 1994. Domains of tau protein and interactions with microtubules. Biochemistry **33:**9511–9522.
38. **Hagiwara, H., H. Yorifuji, R. Sato-Yoshitake, and N. Hirokawa.** 1994. Competition between motor molecules (kinesin and cytoplasmic dynein) and fibrous microtubule-associated proteins in binding to microtubules. J. Biol. Chem. **269:**3581–3589.
39. **Heinlein, M.** 2002. The spread of Tobacco mosaic virus infection: insights into the cellular mechanism of RNA transport. Cell. Mol. Life Sci. **59:**58–82.
40. **Heinlein, M., and B. L. Epel.** 2004. Macromolecular transport and signaling through plasmodesmata. Int. Rev. Cytol. **235:**93–164.
41. **Heinlein, M., B. L. Epel, H. S. Padgett, and R. N. Beachy.** 1995. Interaction of tobamovirus movement proteins with the plant cytoskeleton. Science **270:**1983–1985.
42. **Heinlein, M., H. S. Padgett, J. S. Gens, B. G. Pickard, S. J. Casper, B. L. Epel, and R. N. Beachy.** 1998. Changing patterns of localization of the tobacco mosaic virus movement protein and replicase to the endoplasmic reticulum and microtubules during infection. Plant Cell **10:**1107–1120.
43. **Heinlein, M., M. R. Wood, T. Thiel, and R. N. Beachy.** 1998. Targeting and modification of prokaryotic cell-cell junctions by tobacco mosaic virus cell-to-cell movement protein. Plant J. **14:**345–351.
44. **Hirashima, K., and Y. Watanabe.** 2003. RNA helicase domain of tobamovirus replicase executes cell-to-cell movement possibly through collaboration with its nonconserved region. J. Virol. **77:**12357–12362.
45. **Hirashima, K., and Y. Watanabe.** 2001. Tobamovirus replicase coding region is involved in cell-to-cell movement. J. Virol. **75:**8831–8836.
46. **Hirokawa, N.** 1994. Microtubule organization and dynamics dependent on microtubule-associated proteins. Curr. Opin. Cell Biol. **6:**74–81.
47. **Holt, C. A., R. A. Hodgson, F. A. Coker, R. N. Beachy, and R. S. Nelson.** 1990. Characterization of the masked strain of tobacco mosaic virus: identification of the region responsible for symptom attenuation by analysis of an infectious cDNA clone. Mol. Plant-Microbe Interact. **3:**417–423.
48. **Hugdahl, J. D., and L. C. Morejohn.** 1993. Rapid and reversible high-affinity binding of the dinitroaniline herbicide oryzalin to tubulin of *Zea mays* L. Plant Physiol. **102:**725–740.
49. **Kahn, T. W., M. Lapidot, M. Heinlein, C. Reichel, B. Cooper, R. Gafny, and R. N. Beachy.** 1998. Domains of the TMV movement protein involved in subcellular localization. Plant J. **15:**15–25.
50. **Karpova, O. V., K. I. Ivanov, P. Rodionova, Y. L. Dorokhov, and J. G.**

Atabekov. 1997. Nontranslatability and dissimilar behavior in plants and protoplasts of viral RNA and movement protein complexes formed *in vitro*. Virology **230:**11–21.
51. **Kawakami, S., Y. Watanabe, and R. N. Beachy.** 2004. Tobacco mosaic virus infection spreads cell to cell as intact replication complexes. Proc. Natl. Acad. Sci. USA **101:**6291–6296.
52. **Kirst, M. E., D. J. Meyer, B. C. Gibbon, R. Jung, and R. S. Boston.** 2005. Identification and characterization of endoplasmic reticulum-associated degradation proteins differentially affected by endoplasmic reticulum stress. Plant Physiol. **138:**218–231.
53. **Kiselyova, O. I., I. V. Yaminsky, E. M. Karger, O. Y. Frolova, Y. I. Dorokhov, and J. G. Atabekov.** 2001. Visualization by atomic force microscopy of tobacco mosaic virus movement protein-RNA complexes formed in vitro. J. Gen. Virol. **82:**1503–1508.
54. **Knapp, E., G. M. Danyluk, D. Achor, and D. J. Lewandowski.** 2005. A bipartite Tobacco mosaic virus-defective RNA (dRNA) system to study the role of the N-terminal methyl transferase domain in cell-to-cell movement of dRNAs. Virology **341:**47–58.
55. **Knapp, E., W. O. Dawson, and D. J. Lewandowski.** 2001. Conundrum of the lack of defective RNAs (dRNAs) associated with tobamovirus infections: dRNAs that can move are not replicated by the wild-type virus; dRNAs that are replicated by the wild-type virus do not move. J. Virol. **75:**5518–5525.
56. **Kost, B., and N. H. Chua.** 2002. The plant cytoskeleton: vacuoles and cell walls make the difference. Cell **108:**9–12.
57. **Kotlizky, G., A. Katz, J. van der Laak, V. Boyko, M. Lapidot, R. N. Beachy, M. Heinlein, and B. L. Epel.** 2001. A dysfunctional movement protein of *Tobacco mosaic virus* interferes with targeting of wild type movement protein to microtubules. Mol. Plant-Microbe Interact. **7:**895–904.
58. **Kragler, F., M. Curin, K. Trutnyeva, A. Gansch, and E. Waigmann.** 2003. MPB2C, a microtubule-associated plant protein binds to and interferes with cell-to-cell transport of *Tobacco mosaic virus* movement protein. Plant Physiol. **132:**1870–1883.
59. **Lee, Y. R., H. M. Giang, and B. Liu.** 2001. A novel plant kinesin-related protein specifically associates with the phragmoplast organelles. Plant Cell **13:**2427–2439.
60. **Lichtscheidl, I. K., and F. Baluska.** 2000. Motility of endoplasmic reticulum in plant cells, p. 191–201. *In* C. J. Staiger, F. Baluska, D. Volkmann, and P. W. Barlow (ed.), Actin, a dynamic framework for multiple plant cell functions. Kluwer Academic Publishers, Dordrecht, The Netherlands.
61. **Lloyd, C., and J. Chan.** 2004. Microtubules and the shape of plants to come. Nat. Rev. Mol. Cell Biol. **5:**13–22.
62. **Lloyd, C., and P. Hussey.** 2001. Microtubule-associated proteins in plants–why we need a MAP. Nat. Rev. Mol. Cell Biol. **2:**40–47.
63. **Lopez, L. A., and M. P. Sheetz.** 1993. Steric inhibition of cytoplasmic dynein and kinesin motility by MAP2. Cell Motil. Cytoskeleton **24:**1–16.
64. **Lucas, W. J.** 2006. Plant viral movement proteins: agents for cell-to-cell trafficking of viral genomes. Virology **344:**169–184.
65. **Lucas, W. J., and J. Y. Lee.** 2004. Plasmodesmata as a supracellular control network in plants. Nat. Rev. Mol. Cell Biol. **5:**712–726.
66. **Más, P., and R. N. Beachy.** 1999. Replication of tobacco mosaic virus on endoplasmic reticulum and role of the cytoskeleton and virus movement in intracellular distribution of viral RNA. J. Cell Biol. **147:**945–958.
67. **Más, P., and R. N. Beachy.** 2000. Role of microtubules in the intracellular distribution of tobacco mosaic virus movement protein. Proc. Natl. Acad. Sci. USA **97:**12345–12349.
68. **McLean, B. G., J. Zupan, and P. C. Zambryski.** 1995. Tobacco mosaic virus movement protein associates with the cytoskeleton in tobacco plants. Plant Cell **7:**2101–2114.
69. **Meshi, T., Y. Watanabe, T. Saito, A. Sugimoto, T. Maeda, and Y. Okada.** 1987. Function of the 30 kd protein of tobacco mosaic virus: involvement in cell-to-cell movement and dispensability for replication. EMBO J. **6:**2557–2563.
70. **Moore, P., C. A. Frenczik, C. M. Deom, and R. N. Beachy.** 1992. Developmental changes in plasmodesmata in transgenic tobacco expressing the movement protein of tobacco mosaic virus. Protoplasma **170:**115–127.
71. **Morrissette, N. S., A. Mitra, D. Sept, and L. D. Sibley.** 2004. Dinitroanilines bind alpha-tubulin to disrupt microtubules. Mol. Biol. Cell **15:**1960–1968.
72. **Muller, J., P. Piffanelli, A. Devoto, M. Miklis, C. Elliott, B. Ortmann, P. Schulze-Lefert, and R. Panstruga.** 2005. Conserved ERAD-like quality control of a plant polytopic membrane protein. Plant Cell **17:**149–163.
73. **Murthy, J. V., H. H. Kim, V. R. Hanesworth, J. D. Hugdahl, and L. C. Morejohn.** 1994. Competitive inhibition of high-affinity oryzalin binding to plant tubulin by the phosphoric amide herbicide amiprophos-methyl. Plant Physiol. **105:**309–320.
74. **Nebenfuhr, A., L. A. Gallagher, T. G. Dunahay, J. A. Frohlick, A. M. Mazurkiewicz, J. B. Meehl, and L. A. Staehelin.** 1999. Stop-and-go movements of plant Golgi stacks are mediated by the acto-myosin system. Plant Physiol. **121:**1127–1142.
75. **Nishihama, R., T. Soyano, M. Ishikawa, S. Araki, H. Tanaka, T. Asada, K. Irie, M. Ito, M. Terada, H. Banno, Y. Yamazaki, and Y. Machida.** 2002. Expansion of the cell plate in plant cytokinesis requires a kinesin-like protein/MAPKKK complex. Cell **109:**87–99.
76. **Noueiry, A. O., and P. Ahlquist.** 2003. Brome mosaic virus RNA replication: revealing the role of the host in RNA virus replication. Annu. Rev. Phytopathol. **41:**77–98.
77. **Noueiry, A. O., W. J. Lucas, and R. L. Gilbertson.** 1994. Two proteins of a plant virus coordinate nuclear and plasmodesmal transport. Cell **76:**925–932.
78. **Okita, T. W., and S.-B. Choi.** 2002. mRNA localization in plants: targeting to the cell's cortical region and beyond. Curr. Opin. Plant Biol. **5:**553–559.
79. **Oparka, K. J., D. A. M. Prior, S. Santa Cruz, H. S. Padgett, and R. N. Beachy.** 1997. Gating of epidermal plasmodesmata is restricted to the leading edge of expanding infection sites of tobacco mosaic virus. Plant J. **12:**781–789.
80. **Oparka, K. J., A. G. Roberts, P. Boevink, S. Santa Cruz, I. Roberts, K. S. Pradel, A. Imlau, G. Kotlizky, N. Sauer, and B. Epel.** 1999. Simple, but not branched, plasmodesmata allow the nonspecific trafficking of proteins in developing tobacco leaves. Cell **97:**743–754.
81. **Padgett, H. S., B. L. Epel, T. W. Kahn, M. Heinlein, Y. Watanabe, and R. N. Beachy.** 1996. Distribution of tobamovirus movement protein in infected cells and implications for cell-to-cell spread of infection. Plant J. **10:**1079–1088.
82. **Palacios, I. M., and D. St. Johnston.** 2001. Getting the message across: the intracellular localization of mRNAs in higher eukaryotes. Annu. Rev. Cell Dev. Biol. **17:**569–614.
83. **Panda, D., H. P. Miller, and L. Wilson.** 1999. Rapid treadmilling of brain microtubules free of microtubule-associated proteins in vitro and its suppression by tau. Proc. Natl. Acad. Sci. USA **96:**12459–12464.
84. **Prokhnevsky, A. I., V. V. Peremyslov, and V. V. Dolja.** 2005. Actin cytoskeleton is involved in targeting of a viral Hsp70 homolog to the cell periphery. J. Virol. **79:**14421–14428.
85. **Reichel, C., and R. N. Beachy.** 2000. Degradation of the tobacco mosaic virus movement protein by the 26S proteasome. J. Virol. **74:**3330–3337.
86. **Reichel, C., and R. N. Beachy.** 1998. Tobacco mosaic virus infection induces severe morphological changes of the endoplasmic reticulum. Proc. Natl. Acad. Sci. USA **95:**11169–11174.
87. **Ritzenthaler, C., A. Nebenfuhr, A. Movafeghi, C. Stussi-Garaud, L. Behnia, P. Pimpl, L. A. Staehelin, and D. G. Robinson.** 2002. Reevaluation of the effects of brefeldin A on plant cells using tobacco bright yellow 2 cells expressing Golgi-targeted green fluorescent protein and COPI antisera. Plant Cell **14:**237–261.
88. **Romagnoli, S., G. Cai, and M. Cresti.** 2003. In vitro assays demonstrate that pollen tube organelles use kinesin-related motor proteins to move along microtubules. Plant Cell **15:**251–269.
89. **Romagnoli, S., G. Cai, and M. Cresti.** 2003. Kinesin-like proteins and transport of pollen tube organelles. Cell Biol. Int. **27:**255–256.
90. **Runions, J., T. Brach, S. Kuhner, and C. Hawes.** 2006. Photoactivation of GFP reveals protein dynamics within the endoplasmic reticulum membrane. J. Exp. Bot. **57:**43–50.
91. **Rutten, T., J. Chan, and C. W. Lloyd.** 1997. A 60-kDa plant microtubule-associated protein promotes the growth and stabilization of neurotubules in vitro. Proc. Natl. Acad. Sci. USA **94:**4469–4474.
92. **Seemanpillai, M., R. Elamawi, C. Ritzenthaler, and M. Heinlein.** 2006. Challenging the role of microtubules in *Tobacco mosaic virus* movement by drug treatments is disputable. J. Virol. **80:**6712–6715.
93. **Seitz, A., H. Kojima, K. Oiwa, E. M. Mandelkow, Y. H. Song, and E. Mandelkow.** 2002. Single-molecule investigation of the interference between kinesin, tau and MAP2c. EMBO J. **21:**4896–4905.
94. **Smertenko, A. P., H. Y. Chang, V. Wagner, D. Kaloriti, S. Fenyk, S. Sonobe, C. Lloyd, M. T. Hauser, and P. J. Hussey.** 2004. The Arabidopsis microtubule-associated protein AtMAP65-1: molecular analysis of its microtubule bundling activity. Plant Cell **16:**2035–2047.
95. **Stamer, K., R. Vogel, E. Thies, E. Mandelkow, and E. M. Mandelkow.** 2002. Tau blocks traffic of organelles, neurofilaments, and APP vesicles in neurons and enhances oxidative stress. J. Cell Biol. **156:**1051–1063.
96. **Takamatsu, K., M. Ishikawa, T. Meshi, and Y. Okada.** 1987. Expression of bacterial chloramphenicol acetyltransferase gene in tobacco plants mediated by TMV-RNA. EMBO J. **6:**307–311.
97. **Tanaka, H., M. Ishikawa, S. Kitamura, Y. Takahashi, T. Soyano, C. Machida, and Y. Machida.** 2004. The AtNACK1/HINKEL and STUD/TETRASPORE/AtNACK2 genes, which encode functionally redundant kinesins, are essential for cytokinesis in Arabidopsis. Genes Cells **9:**1199–1211.
98. **Trinczek, B., A. Ebneth, E. M. Mandelkow, and E. Mandelkow.** 1999. Tau regulates the attachment/detachment but not the speed of motors in microtubule-dependent transport of single vesicles and organelles. J. Cell Sci. **112:**2355–2367.
99. **Van Damme, D., K. Van Poucke, E. Boutant, C. Ritzenthaler, D. Inzé, and D. Geelen.** 2004. In vivo dynamics and differential microtubule-binding activities of MAP65 proteins. Plant Physiol. **136:**3956–3967.
100. **Vandecandelaere, A., B. Pedrotti, M. A. Utton, R. A. Calvert, and P. M. Bayley.** 1996. Differences in the regulation of microtubule dynamics by microtubule-associated proteins MAP1B and MAP2. Cell Motil. Cytoskeleton **35:**134–146.

101. **Vetter, G., J. M. Hily, E. Klein, L. Schmidlin, M. Haas, T. Merkle, and D. Gilmer.** 2004. Nucleo-cytoplasmic shuttling of the beet necrotic yellow vein virus RNA-3-encoded p25 protein. J. Gen. Virol. **85:**2459–2469.
102. **von Massow, A., E. M. Mandelkow, and E. Mandelkow.** 1989. Interaction between kinesin, microtubules, and microtubule-associated protein 2. Cell Motil. Cytoskeleton **14:**562–571.
103. **Waigmann, E., W. Lucas, V. Citovsky, and P. Zambryski.** 1994. Direct functional assay for tobacco mosaic virus cell-to-cell movement protein and identification of a domain involved in increasing plasmodesmal permeability. Proc. Natl. Acad. Sci. USA **91:**1433–1437.
104. **Walker, R. A., N. K. Pryer, and E. D. Salmon.** 1991. Dilution of individual microtubules observed in real time in vitro: evidence that cap size is small and independent of elongation rate. J. Cell Biol. **114:**73–81.
105. **Wicker-Planquart, C., V. Stoppin-Mellet, L. Blanchoin, and M. Vantard.** 2004. Interactions of tobacco microtubule-associated protein MAP65-1b with microtubules. Plant J. **39:**126–134.
106. **Wilson, L., H. P. Miller, K. W. Farrell, K. B. Snyder, W. C. Thompson, and D. L. Purich.** 1985. Taxol stabilization of microtubules in vitro: dynamics of tubulin addition and loss at opposite microtubule ends. Biochemistry **24:**5254–5262.
107. **Wolf, S., C. M. Deom, R. N. Beachy, and W. J. Lucas.** 1989. Movement protein of tobacco mosaic virus modifies plasmodesmatal size exclusion limit. Science **246:**377–379.
108. **Xoconostle-Cazares, B., Y. Xiang, R. Ruiz-Medrano, H. L. Wang, J. Monzer, B. C. Yoo, K. C. McFarland, V. R. Franceschi, and W. J. Lucas.** 1999. Plant paralog to viral movement protein that potentiates transport of mRNA into the phloem. Science **283:**94–98.
109. **Yang, Y. D., R. Elamawi, J. Bubeck, R. Pepperkok, C. Ritzenthaler, and D. G. Robinson.** 2005. Dynamics of COPII vesicles and the Golgi apparatus in cultured Nicotiana tabacum BY-2 cells provides evidence for transient association of Golgi stacks with endoplasmic reticulum exit sites. Plant Cell **17:**1513–1531.
110. **Zambryski, P.** 1995. Plasmodesmata: plant channels for molecules on the move. Science **270:**1943–1944.